

Care for the Mind Amid Chronic Diseases: An Interpretable AI Approach Using IoT

Jiaheng Xie^{1,**}, Xiaohang Zhao^{2,**,*}, Xiang Liu¹, Xiao Fang¹

¹ Lerner College of Business and Economics,
University of Delaware, Newark, DE, USA

² School of Information Management & Engineering,
Shanghai University of Finance and Economics, Shanghai, China

* Corresponding Author: Xiaohang Zhao, xiaohangzhao@mail.shufe.edu.cn

** Equal Contribution

Abstract: Health sensing for chronic disease management creates immense benefits for social welfare. Existing health sensing studies primarily focus on the prediction of physical chronic diseases. Depression, a widespread complication of chronic diseases, is however understudied. We draw on the medical literature to support depression prediction using motion sensor data. To connect human expertise in the decision-making, safeguard trust for this high-stake prediction, and ensure algorithm transparency, we develop an interpretable deep learning model: Temporal Prototype Network (TempPNet). TempPNet is built upon the emergent prototype learning models. To accommodate the temporal characteristic of sensor data and the progressive property of depression, TempPNet differs from existing prototype learning models in its capability of capturing the temporal progression of depression. Extensive empirical analyses using real-world motion sensor data show that TempPNet outperforms state-of-the-art benchmarks in depression prediction. Moreover, TempPNet interprets its predictions by visualizing the temporal progression of depression and its corresponding symptoms detected from sensor data. We further conduct a user study to demonstrate its superiority over the benchmarks in interpretability. This study offers an algorithmic solution for impactful social good — collaborative care of chronic diseases and depression in health sensing. Methodologically, it contributes to extant literature with a novel interpretable deep learning model for depression prediction from sensor data. Patients, doctors, and caregivers can deploy our model on mobile devices to monitor patients’ depression risks in real-time. Our model’s interpretability also allows human experts to participate in the decision-making by reviewing the interpretation of prediction outcomes and making informed interventions.

Keywords: interpretable AI, prototype learning, algorithm transparency, temporal prototype network, depression prediction, motion sensor, human evaluation, social good

1. Introduction

Chronic diseases are a dire global problem with grand societal and economic impacts. In the US alone, 129 million Americans suffer from one or more chronic diseases (Anderson 2010), of which the most common ones are heart diseases, cancer, Alzheimer’s, and diabetes (CDC 2022). The population of chronic disease patients is expected to increase by over 10 million per decade (Anderson 2010). Moreover, treatments of chronic diseases account for 90% of the US’s \$3.8 trillion annual healthcare cost (CDC 2021). Such serious consequences of chronic diseases demand high-quality intelligent chronic care (Dixon-Woods et al. 2013).

Among intelligent chronic care technologies, sensing technologies have pioneered the healthcare digital transformation, due to the ubiquity of smartphones and smartwatches (Dadkhah et al. 2021). Most of these devices are equipped with motion sensors, such as accelerometers and gyroscopes, which can collect an immense amount of high-fidelity patient motion data in real-time. Recognizing the potential of these sensing technologies, prior studies have leveraged them in copious applications, such as vital sign assessment (Dias and Cunha 2018), Alzheimer’s diagnosis (Laplante and Laplante 2015), sleep monitoring (Lee et al. 2015), and fall detection (Mozaffari et al. 2019). Riding on this cutting-edge revolution, the information systems (IS) discipline has also been pushing forward for the adoption of sensing technologies to support chronic disease management, apart from the conventional use of electronic health records (EHR) and health social media (Bardhan et al. 2017, Karahanna et al. 2020). For example, a few recent IS studies have resorted to motion sensors for Parkinson’s disease management (Yu et al. 2022) and daily activity recognition (Zhu et al. 2021).

While treatments of chronic diseases attract the primary research efforts, care for depression associated with chronic diseases has not received due attention, although medical experts have repeatedly stressed the urgency of collaborative care for depression and chronic diseases (Katon et al. 2010). Depression is epidemic among chronic disease patients, caused by frustrating long-haul symptoms and complex home regimens. Evidence shows that depression occurs in 17% of cardiovascular cases, 23% of cerebrovascular cases, 27% of diabetes patients, and 40% of cancer patients (CDC 2012). According to the National Institutes of Health (NIH), chronic disease patients are twice as likely to suffer from depression as the general population, and depression could drastically elevate chronic disease severity (NIH 2022). Therefore, mental care amid chronic disease is essential. Accordingly, our first objective is to *predict the occurrence of depression for chronic disease patients using sensing technologies*. When early signs of depression are detected, our model could alert caregivers and doctors to actively intervene and treat chronic disease patients’ mental disorders.

A key challenge of using sensing technologies to predict depression is that motion sensors only capture patients’ physical movements, while depression is a disorder of mental activity. Nevertheless, medical studies have shown that depression presents many physical symptoms, such as moving or speaking more slowly than usual, unexplained aches and pains, and lack of energy (NHS 2022, Sloman et al. 1982, Lemke et al. 2000). Such physical symptoms of depression are embodied in walking patterns that can be captured by motion sensors. These medical discoveries that connect physical movements and depression lay the foundation for our prediction of depression from motion sensor data.

Due to the high stake and impact of healthcare predictions, a black-box prediction model is inadequate. Interpretability is essential to increase trust in a prediction model, prevent failures, and justify its usage (Moss et al. 2022). Moreover, the output of a depression prediction model is reviewed and used by medical experts. An interpretable model allows them to understand the reasoning behind the prediction and make professional diagnoses and accurate interventions. Therefore, our second objective is to *build an interpretable model for depression prediction*. As mentioned above, the medical literature finds that depressed patients present typical walking symptoms (NHS 2022). Therefore, these walking symptoms discovered from sensor data serve as a natural interpretation mechanism for the prediction of depression.

Recognizing patterns in the input to interpret machine learning (ML) predictions forms a research forefront: prototype learning, which was originally proposed to interpret the classification of images (Chen et al. 2019). When interpreting how to classify an image, one focuses on parts of the image and compares them with prototypical images from a given class. For instance, radiologists compare suspected tumors in X-rays with prototypical tumor images for the diagnosis of cancer (Chen et al. 2019). The resemblance of an input image to a prototypical class is the mechanism to interpret the classification of the image. In this study, typical depression walking symptoms captured in motion sensor data can be recognized as prototypes to interpret depression prediction. Existing prototype learning methods, however, are inadequate for our study because of the following challenges. First, existing methods predict and interpret from a single input (e.g., an image). In contrast, we need to design a method that can predict and interpret from a sequence of inputs (i.e., sequential motion data). Second, the severity of depression symptoms evolves over time, such as trending up, peaking, and flattening (Dattani et al. 2021). Static prototypes defined by existing prototype learning methods cannot capture such dynamic and temporal patterns of depression symptom evolution. Accordingly, we need to define a novel temporal prototype that can capture such dynamic patterns and design a new prototype learning method that can learn temporal prototypes from motion sensor data.

In sum, this study targets the interpretable prediction of depression associated with chronic diseases and makes the following contributions. From the methodological perspective, we propose a novel interpretable deep learning method for depression prediction from motion sensor data. Different from state-of-the-art prototype learning methods, our method takes sequential motion sensor data as inputs and innovatively learns two kinds of prototypes from the data: prototypes of depression symptoms and prototypes of temporal symptom progression. It then predicts the depression status of a chronic disease patient and interprets the prediction based on these two kinds of prototypes. Extensive empirical analyses using real-world motion sensor data demonstrate the superior predictive power of our method over state-of-the-art benchmark methods. Through a user study, we also show that our method outperforms these benchmarks in terms of interpretability. From the practical perspective, our proposed method can be implemented as a mobile application, which is able to predict and monitor chronic disease patients' depression risk in real-time based on motion sensor data collected by their mobile devices. Once our method detects early signs of depression, it can send alerts to caregivers and doctors to provide timely treatments, such as antidepressants and social support groups.

2. Literature Review

Our study is related to two streams of research. We first review existing health sensing studies and identify the opportunities from the domain perspective in Section 2.1. Next, in Section 2.2, we survey interpretable ML methods with a focus on prototype learning methods because they represent the state-of-the-art developments in interpretable ML and are particularly related to our study methodologically. We discuss the key novelties of our study in comparison to the literature in Section 2.3.

2.1. Health Sensing and Depression

As wearable devices become ubiquitous, motion sensors, such as accelerometers and gyroscopes, have attracted extensive research attention to collect high-fidelity, real-time motion data for intelligent chronic disease management. Table 1 summarizes recent health sensing studies. These studies typically recruit a cohort of patients to conduct walking tests, whose sample sizes range from 12 to 683 participants (Coelln et al. 2019). During a walking test, a participant is instructed to walk for a certain distance while his or her walking signals are recorded by motion sensors. Using walking sensor data as the input, existing studies have applied machine and deep learning methods, such as convolutional neural networks (CNNs), support vector machines (SVMs), and random forests (RFs), to predict the occurrence and severity of chronic diseases.

While the prediction of chronic diseases, such as Parkinson's disease (PD) and diabetes, deserve research attention in the health sensing discipline, mental care is equally critical to chronic care.

Table 1 Summary of Recent Health Sensing Studies

Study	Data	Number of Subjects	Task	Model
Anand and Stepp (2015)	Walking tests	25	PD detection	Regression, NB, RF
Um et al. (2017)	Walking tests	30	PD motor detection	CNN
Millor et al. (2017)	Walking tests	431	Frailty prediction	Decision tree
Watanabe et al. (2017)	Walking tests	12	Diabetes forefoot load detection	Statistical analysis
Polat (2019)	Walking tests	16	PD prediction	Regression
Coelln et al. (2019)	Walking tests	683	PD prediction	Cox
Rastegari et al. (2019)	Walking tests	43	PD diagnosis	SVM, RF, NB, AdaBoost
Nemati et al. (2020)	Cough and speech	21	Lung disease prediction	Regression, SVM, RF, MLP
Moon et al. (2020)	Walking tests	524	PD prediction	NN, SVM, KNN, decision tree, RF
Piau et al. (2020)	Walking tests	125	Fall detection	Regression

This is because irritating physical symptoms and tedious long-term disease management cause serious mental complications. Studies have shown that clinically significant depressive disturbances occur in 40-50% of chronic disease patients (Reijnders et al. 2008). Despite such a high rate of occurrence, depression is treatable and recovery is possible (Marsh 2013). On the flip side, if depression is left untreated, its impact could extend far beyond mental symptoms, including greater functional disability, faster physical and cognitive deterioration, increased mortality, poorer quality of life, and increased caregiver distress (Marsh 2013). In this study, *we aim to predict the occurrence of depression for chronic disease patients using motion sensor data.*

Medical studies have provided abundant evidence that motion symptoms are an essential manifestation of depression. Sloman et al. (1982) find that depressed patients' walks are slower, and the lifting motion of the leg is slower, compared to healthy people. Lemke et al. (2000) show that depressed patients have shorter strides and slower gait velocity than healthy people. Michalak et al. (2009) discover that depressed patients exhibit reduced vertical head movements, more slumped posture, and lower gait velocity. Clinical studies have also proven that these physical depression symptoms can be reliably captured via self-conducted walking tests (Vancampfort et al. 2020). This is because these patients suffer from major depressive disorder instead of temporary mood swings. Major depressive disorder is persistent and causes significant impairment in daily life (Mayo Clinic 2022). For such a persistent disorder, the above-mentioned walking symptoms will be present in walking tests.

Related to this study, several prior works also recognize the opportunity of predicting depression based on mobility data. Canzian and Musolesi (2015) use GPS mobility traces to predict a patient's depressive state using SVM. Jacobson and Chung (2020) conduct a study of 31 patients and employ XGBoost to predict their depressive status based on sensor data collected from these patients.

Farhan et al. (2016) recruit 79 participants for sensor data collection and predict their occurrence of depression using regression. Our study differs from these studies in the following aspects. First, these studies employ conventional ML methods, such as SVM, XGBoost, and regression, which have been shown to be less effective in various applications compared to deep learning models (Xie et al. 2022, Yu et al. 2022, Zhu et al. 2021). Due to the high impact of this area and the rapid advances in deep learning, the computational methods for sensor-based depression prediction are due a much-needed, timely revisit and upgrade. Second, because of their use of conventional ML methods, these studies have to craft features from sensor data. Such manual design and selection of features are labor-intensive, require significant domain knowledge, and could lead to inconclusive results (Hubble et al. 2015, Yu et al. 2022). Third, the intention of these models is to make predictions, not interpretations. Therefore, they are either black-box models or models that explain predictions based on simple, hand-crafted features from sensor data, such as mean and variance. These features are primitive and not unique to depression, thus falling short of offering a meaningful and practical interpretation. In order for end users (e.g., doctors, patients, and caregivers) to trust and adopt a prediction model, meaningful interpretation is the key. Interpretation also brings extensive value to ML. The most significant one is social acceptance, which is required to integrate algorithms into daily lives (Xie and Liu 2020). As our society is progressing toward integration with ML, new regulations have been imposed to require verifiability, accountability, and more importantly, full transparency of algorithm decisions. A key example is the European General Data Protection Regulation (GDPR), which requires companies to provide data subjects the right to an explanation of algorithm decisions. Consequently, *we aim to propose a novel interpretable deep learning model for depression prediction.*

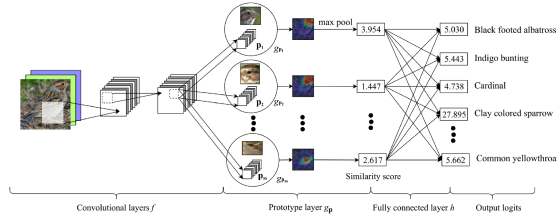
2.2. Interpretable Machine Learning and Prototype Learning

The majority of interpretable ML methods offer feature-based interpretation, where handcrafted features are required, and their interpretation reveals the attribution of each feature to the prediction. These methods can be post-hoc, such as SHAP and LIME (Lundberg and Lee 2017), or model-based, such as generative additive model (GAM) (Caruana et al. 2015) and wide and deep learning (W&D) (Xie and Liu 2020). Post-hoc models use an additive feature explanation model, which is a linear function of binary variables: $g(z') = \phi_0 + \sum_{i=1}^M \phi_i z'_i$, where ϕ_i is the attribution of a feature to the prediction, and z'_i is the binary indicator of a feature (Lundberg and Lee 2017). Model-based interpretable methods have a built-in interpretation component within the prediction model. For example, GAM’s outcome variable depends linearly on the smooth functions of predictors, with an interest focusing on the inference of these smooth functions (Caruana et al. 2015). W&D trains an interpretable linear component jointly with a deep neural network. The

linear component produces a weight for each feature to interpret the feature importance (Cheng et al. 2016).

Feature-based interpretable methods fall short in interpreting sensor-based predictions, because it is intrinsically challenging to design meaningful and effective features from sensor signals. Although a few studies crafted simple sensor-based features — such as mean, variance, and standard deviation of a segment of signals (Oung et al. 2015) — they do not characterize the uniqueness of depression. Besides, manually engineering meaningful features from sensor signals requires intensive labor and could even result in inconclusive results (Hubble et al. 2015, Yu et al. 2022). Such a practice also demands rich domain knowledge, which is not easily accessible (Yu et al. 2022). Fortunately, medical literature reveals that depressed patients present typical walking symptoms (Sloman et al. 1982, Lemke et al. 2000, NHS 2022). Without feature engineering, these walking symptoms can be fruitfully leveraged to interpret the prediction of depression. For that purpose, an emergent line of interpretable ML research, prototype learning, has been proposed to utilize the prototypical part of a class (prototype) to interpret the prediction. For instance, a prototypical depression walking symptom learned from sensor signals can interpret why a patient is classified as depressed.

Prototype learning was originally proposed to interpret image recognition (Chen et al. 2019). A motivating example is that when humans describe why a bird picture is classified as a clay-colored sparrow, we might reason that the bird’s head and wing bars look like those of a prototypical clay-colored sparrow. Leveraging such a reasoning mechanism, Chen et al. (2019) devise ProtoPNet (Figure 1a). To classify a bird picture into a particular bird species with interpretation, this model introduces a prototype layer where K prototypes are assigned to each known species. Each of these prototypes is intended to capture the prototypical parts, or the most salient and typical representation, of the corresponding bird species, such as the head of a clay-colored sparrow or the wing of a cardinal. ProtoPNet embeds each prototype j as a vector p_j in the latent space, and defines *prototype similarity* s_j to measure how strongly prototype j exists in the input bird picture by comparing p_j and the feature maps (extracted via convolutional layers) of the picture in the latent space. The model subsequently classifies the input bird picture based on the weighted sum of the prototype similarities computed between this picture and each prototype. ProtoPNet visualizes each prototype as the most relevant region of the bird picture where the prototype most strongly exists, and interprets why it thinks the input bird picture should be classified as a particular species by identifying several parts from the picture that look like the prototypical parts (prototypes) of the species.



(a) ProtoPNet (Chen et al. 2019)

Input: excellent food . extremely clean . the staff is friendly and efficient . really good atmosphere .
 Prediction: Positive(1.00)
 Explanation:
 (0.86) EXCELLENT FOOD . NICE decor . a little pricey for the proportions . the salmon WAS AMAZING . -> Positive(1.58)
 (0.68) GREAT FOOD SERVICE and views . hard to beat . this is our FAVORITE <other> restaurant in the valley . -> Positive(1.23)
 (0.50) GREAT FOOD GREAT SERVICE . vietnamese <other> rolls unbelievable . GREAT food just what the neighborhood needed . -> Positive(2.82)

(b) ProSeNet Example (Ming et al. 2019)

Figure 1 Existing Prototype Learning Models

Prototype learning has been extended to interpret text classification. In this vein, Ming et al. (2019) propose ProSeNet, which adds the prototype layer after the sequence encoder (e.g., RNN). This model is able to predict the class of a sentence (e.g., positive or negative) and explain which part of the sentence (prototype) leads to such a prediction result. Figure 1b shows an example, where the input is classified as positive because it strongly presents positive prototypes, such as “excellent food” and “great food service.” A number of prototype learning models have also been proposed for various tasks. For example, Rymarczyk et al. (2021) develop ProtoPShare that captures sharing property between each pair of prototypes. Nauta et al. (2021a) combine decision trees and prototype learning so that the prototype reasoning process can be streamlined as a tree structure. Singh and Yow (2021) design two groups of prototypes: one group that the input looks like and the other group that the input does not look like. Table 2 contrasts major prototype learning methods with our method.

2.3. Key Novelties of Our Study

Our literature review reveals several research gaps and opportunities for methodological innovation. Prior health sensing research mostly focuses on chronic disease prediction but generally overlooks depression prediction. Although a few studies attempt to predict depression using mobility and sensor data, they are ML-based and are either black-box models or models that explain predictions based on simple features (e.g., mean and variance) of sensor data, which are undesired for healthcare applications. Different from these studies, our research devises a novel interpretable deep learning model for depression prediction, following the cutting-edge prototype learning paradigm.

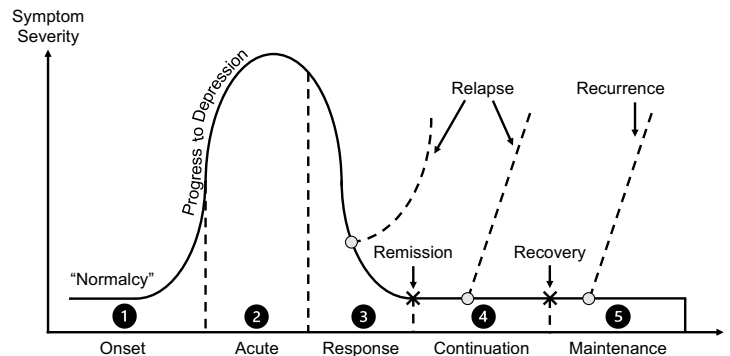
Although existing prototype learning methods offer an exciting mode of prediction and interpretation, they fall short in the present study. These methods make predictions and interpretations from a single input (e.g., an image or a sentence) and define their prototypes for individual components of that input (e.g., the head of a clay-colored bird). In contrast, our method takes a sequence of inputs because each patient performs a sequence of walking tests. The temporal dimension of our method’s inputs has practical implications because medical literature suggests that depression symptoms are progressive and have multiple phases (Bockting et al. 2015, Dattani et al. 2021). As

Table 2 Existing Prototype Learning Methods vs. Our Method

Study	Model	Novelty	Input	TP*
Chen et al. (2019)	ProtoPNet	Prototype for image classification	An image	No
Hase et al. (2019)	HPNet	Hierarchical prototype	An image	No
Ming et al. (2019)	ProSeNet	Prototype for text classification	A piece of text	No
Xu et al. (2020b)	APN	Represent attribute for zero-shot learning	An image	No
Shitole et al. (2021)	Structured Attention Graphs	Attention maps to explain a classifier	An image	No
Rymarczyk et al. (2021)	ProtoPShare	Prototype parts share	An image	No
Nauta et al. (2021a)	ProtoTree	Prototype and decision tree	An image	No
Wang et al. (2021b)	TesNet	Add embedding space using manifold	An image	No
Singh and Yow (2021)	NP-ProtoPNet	Positive reasoning and negative reasoning	An image	No
Nauta et al. (2021b)	Explain ProtoPNet	Generate textual info about prototypes	An image	No
Our Method	TempPNet	Capture temporal progression of the input	A sequence of walking tests	Yes

* TP stands for “Temporal Progression”, indicating whether a model is capable of detecting interpretable temporal progression patterns from its input and then leveraging these patterns for prediction and interpretation. We articulate this point in Section 2.3.

depicted in Figure 2, from the onset phase, a patient’s symptom severity may trend up and progress to acute depression. After the acute phase, some patients’ symptoms may peak and flatten, while others could exacerbate. A portion of the patients may recover from depression, and their symptom severity trends down. At any timepoint, a recovered patient is likely to relapse, and symptoms will subsequently recur and their severities may fluctuate.

**Figure 2 Temporal Progression of Depression (Bockting et al. 2015)**

When applying existing prototype learning methods to our study, we are able to determine to what extent a single walking test is “normal”. However, no depression symptom in a single walking

test does not imply that the patient has no depression because the test might be performed at the “normalcy phase,” which could just be transitory and would quickly progress to severe depression. As a result, it is essential to predict and interpret the mental state of a patient based on a temporal sequence of walking tests that characterizes the full course of symptom progression. Motivated by this fact and the depression progression literature (Bockting et al. 2015, Dattani et al. 2021), we aim to design a novel prototype learning method that predicts and interprets the occurrence of depression based on prototypical temporal symptom progression detected from walking test sequences.

3. Problem Formulation

For a patient u , let $y^{(u)}$ be the patient’s depression status, where $y^{(u)} = 1$ denotes depression, and $y^{(u)} = 0$ represents non-depression. We also observe this patient’s N_u walking tests denoted by $X^{(u)} = \langle X_1^{(u)}, X_2^{(u)}, \dots, X_{N_u}^{(u)} \rangle$ that are performed at timepoints $\langle t_1^{(u)}, t_2^{(u)}, \dots, t_{N_u}^{(u)} \rangle$. Each walking test is comprised of three tasks: walking outbound for 30 seconds, returning to the original place, and standing for 30 seconds. The i th walking test $X_i^{(u)}$ observed at timepoint $t_i^{(u)}$ (e.g., 2015-05-04) is comprised of a sequence of regularly sampled sensor data: $X_i^{(u)} = \langle a_1, a_2, \dots, a_L \rangle$, where vector a_l is the sensor feature sampled at timepoint l (e.g., 1850 milliseconds after the start of the walking test).¹ Each sensor feature a_l is derived from the accelerometer readings and gyroscope readings recorded for the three tasks in the walking test. Please see Appendix A for the details of a_l .

Let \mathcal{U} denote the set of patients. We observe the dataset $\mathcal{D} = \{(X^{(u)}, y^{(u)}) | u = 1, 2, \dots, |\mathcal{U}|\}$, where $X^{(u)}$ and $y^{(u)}$ represent the sequence of walking tests and the depression status of patient u , respectively, and $|\mathcal{U}|$ denotes the number of patients. The objective of the problem studied is to learn a model from \mathcal{D} that can predict the depression status of a new patient, based on sensor data collected from the patient’s walking tests, and interpret the prediction. Table 3 summarizes the important notations used in this paper.

To solve this problem, it is critical to learn two kinds of prototypes from \mathcal{D} : symptom prototypes (e.g., short strides and slow gait velocity) and trend prototypes (e.g., symptom severity trending up, trending down, and fluctuating). To learn these prototypes, we need to tackle three methodological challenges. First, while rich sensor data can be collected during a walking test, it is non-trivial to define prototypes representing depression symptoms, such that their existing strength² in a walking test can be interpreted as the snapshot of symptom severity at the time of the walking test. Second,

¹In our context, sensor signals are sampled with a fixed frequency. For example, a sampling frequency of 100Hz means that one sensor feature vector is collected per 0.01 second. To simplify notation, we omit the specificity to walking test and patient in notation a_l (a sensor feature) and L (the length of a sensor signal sequence). Note that different sensor signal sequences could have different lengths.

²Existing strength is defined as how strongly a depression symptom presents in a walking test.

the elapsed time between two consecutive walking tests is irregular. For example, a patient might take the second walking test one day after the first one, while taking the third test four days after the second one. On the one hand, it is essential to explicitly consider these irregular inter-test time intervals when inspecting the time series of symptom severities, because they reveal the progression of symptom severities and enable the definition of prototypes representing temporal depression symptom progression. On the other hand, existing prototype learning methods cannot deal with sequential inputs that are irregularly spaced in time, as indicated by the TP column in Table 2. This gap motivates us to develop a novel and effective method to analyze this new type of input for prototype learning. Lastly, different patients often conduct varying numbers of walking tests within an observation time window. It is also unknown which phase of depression progression each walking test is performed at. Consequently, given a prototypical temporal symptom progression, it is difficult to measure its existing strength in a walking test sequence because the two objects are not aligned in time. That is, for each walking test, we do not know against which part of the prototypical progression the walking test should be compared. In the next section, we develop a novel method that explicitly addresses these three challenges.

Table 3 Notation

Notation	Description
X_i	The sensor signal sequence of the i th walking test of a focal patient.
t_i	The timepoint when the walking test X_i is performed.
H_i^S	The feature matrix extracted from walking test X_i .
p_m^S	The embedding vector for symptom prototype m .
$s_{m,i}^S$	The existence strength of symptom prototype m in walking test X_i , or the severity of symptom m detected in the walking test, defined by Equation 2.
S	The symptom progression matrix detected for the focal patient, defined by Equation 3.
$\mathcal{G}^{(k)}(t)$	The definition of trend prototype k , defined by Equation 6.
s_k^T	The existence strength of trend prototype k in symptom progression matrix S , defined by Equation 9.

4. The TempPNet Approach

To overcome the above-mentioned technical challenges, we present the Temporal Prototype Network (TempPNet), an interpretable classifier equipped with a novel temporal prototype layer that predicts depression status based on the prototypical temporal progression of walking symptoms. Figure 3 shows the architecture of our model, which features three building blocks: a feature extraction layer that represents a sequence of walking tests as a sequence of features, a temporal prototype layer that defines symptom prototypes and trend prototypes for depression detection and then computes the existing strength of these prototypes in a walking test sequence, and lastly a classification layer that classifies a patient into depression or non-depression categories based on

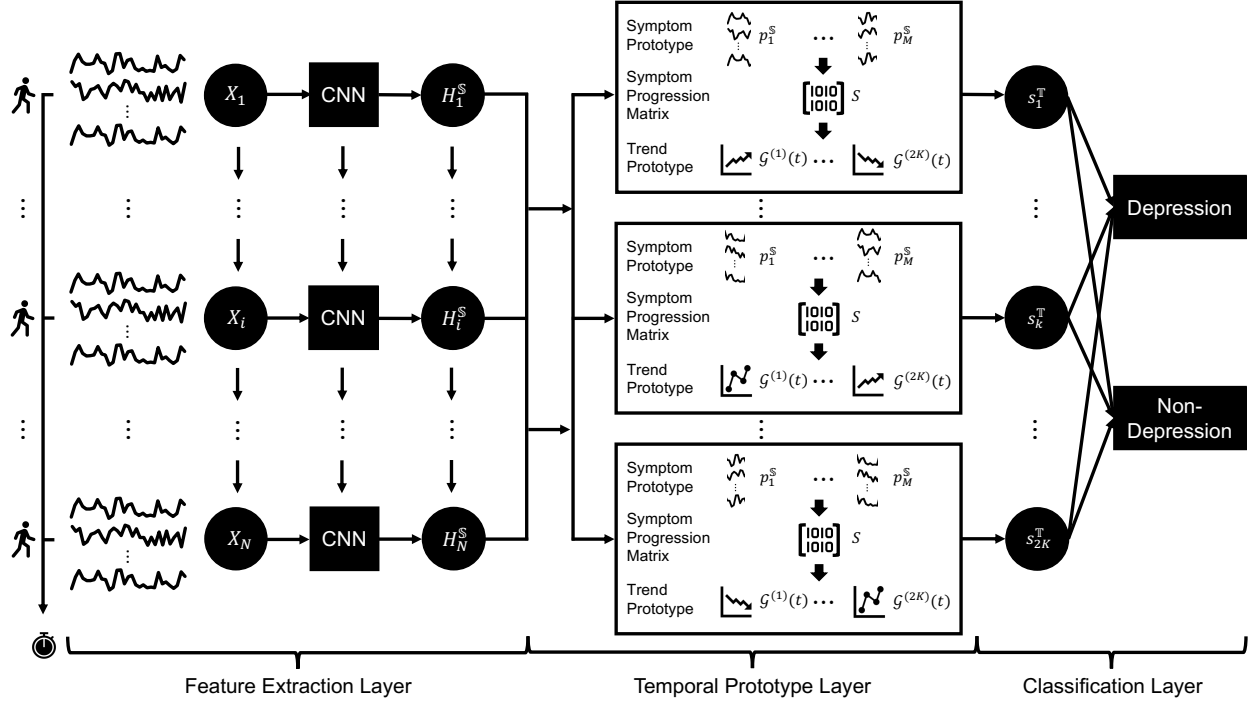


Figure 3 TempPNet Architecture

the existing strength of trend prototypes. We organize the method description as follows. Section 4.1 introduces the feature extraction layer and the symptom prototypes, based on which we propose the symptom progression matrix, the foundational artifact of TempPNet. Next, we proceed to the design of the trend prototypes in Section 4.2 for detecting prototypical symptom progression patterns of depression state. We then finish the development of TempPNet in Section 4.3 by specifying the classification layer and the learning objective.

4.1. The Symptom Prototype and Symptom Progression Matrix

In the following discussion, we consider a focal patient u , and thus drop the superscripts and subscripts related to the patient to simplify the notation. Recall that we can observe a sequence of N walking tests for this patient, whose i th walking test is represented by the sensor signal sequence X_i . To learn an effective representation of X_i , we employ a deep Convolutional Neural Network (CNN) layer (Goodfellow et al. 2016, Zhang et al. 2020). Let $H_i^S \in R^{n_o \times n_e}$ denote the learned embedding matrix for the sensor signal sequence X_i , where n_o is the number of patches generated by the deep CNN layer and n_e is the embedding dimension of each patch (Chen et al. 2019). We define H_i^S as

$$H_i^S = \text{CNN}(X_i) \quad (1)$$

where the specifications of the deep CNN layer are articulated in Appendix B. Let $H_{o|i}^{\mathbb{S}}$ denote the o th column of $H_i^{\mathbb{S}}$. The key benefit of using CNN for learning the embedding of X_i is that each patch $H_{o|i}^{\mathbb{S}}$ has its own receptive field,³ which can be identified and visualized as a local segment in X_i . Following Chen et al. (2019), we identify the symptoms at the receptive field level. We articulate how to leverage this property to inspect the learned prototypes in Section 4.4. Equation 1 corresponds to the feature extraction layer of TempPNet in Figure 3.

Similar to prototype learning in image recognition, we aim to detect what prototypical walking symptoms $H_i^{\mathbb{S}}$ (the representation of X_i) resembles. For this purpose, we need to learn M symptom prototypes that represent typical walking symptoms, such as short strides and slow gait velocity (Lemke et al. 2000, Michalak et al. 2009, Czech and Patel 2019). These symptom prototypes are defined as the latent representation of prototypical waking patterns in the input signal. We embed each symptom prototype m as a vector $p_m^{\mathbb{S}} \in R^{n_e}$ for $m = 1, 2, \dots, M$, which is in the same latent space as $H_i^{\mathbb{S}}$. Following the common strategy of prototype learning (Chen et al. 2019), symptom prototype vector $p_m^{\mathbb{S}}$ will be learned as model parameters, and then identified as and visualized by the walking test segment where it presents most strongly. The interpretation mechanism is to find the prototypical patterns within the input sensor signal that are indicative of depression walking symptoms and thereby informative for depression prediction. The middle part of Figure 3 provides an exemplar visualization of the symptom prototypes. Let $s_{m,i}^{\mathbb{S}}$ denote the existing strength of symptom prototype m in walking test X_i , which can also be understood as the severity of symptom m detected in the walking test. We define $s_{m,i}^{\mathbb{S}}$ as

$$s_{o|m,i}^{\mathbb{S}} = \exp(\gamma - \|H_{o|i}^{\mathbb{S}} - p_m^{\mathbb{S}}\|_2^2) \quad (2a)$$

$$s_{m,i}^{\mathbb{S}} = \max_{o=1,2,\dots,n_o} s_{o|m,i}^{\mathbb{S}} \quad (2b)$$

where $\gamma < 0$ is an infinitesimal constant to ensure $0 < s_{o|m,i}^{\mathbb{S}} < 1$ for $o = 1, 2, \dots, n_o$. A high value of $s_{o|m,i}^{\mathbb{S}}$ suggests that strong existence of symptom prototype m , or high severity of walking symptom m , is detected in the o th region in walking test X_i . As a result, $s_{m,i}^{\mathbb{S}}$ measures the overall severity of symptom prototype m in walking test X_i .

Unlike existing prototype learning studies that predict and interpret based on static prototypes solely (Chen et al. 2019, Ming et al. 2019), the severity of symptom prototype $s_{m,i}^{\mathbb{S}}$ is dynamic and forms a temporal progression pattern, as we observe patients' sensor data over time. By collecting

³A receptive field is the region in which an optimal stimulus elicits vigorous response from a neuron (Goodfellow et al. 2016)

the severity scores of all symptom prototypes across the sequence of walking tests, we can construct the symptom progression matrix $S \in R^{M \times N}$ as

$$S = \begin{array}{cccc} & t_1 & t_2 & \dots & t_N \\ \begin{array}{c} \text{sym}_1 \\ \text{sym}_2 \\ \vdots \\ \text{sym}_M \end{array} & \begin{bmatrix} s_{1,1}^S & s_{1,2}^S & \dots & s_{1,N}^S \\ s_{2,1}^S & s_{2,2}^S & \dots & s_{2,N}^S \\ \vdots & \vdots & \ddots & \vdots \\ s_{M,1}^S & s_{M,2}^S & \dots & s_{M,N}^S \end{bmatrix} & & & \end{array} \quad (3)$$

where we label each column by the timepoint when the corresponding walking test is performed, and each row by the corresponding symptom prototype (sym_m denotes symptom m). In matrix S , the m th row corresponds to the temporal progression of the severities of symptom m , while the i th column corresponds to the *contemporaneous distribution of symptom severities* observed at timepoint t_i . In other words, if we regard each symptom severity as a random variable that randomly evolves over time, then the column vector S_i is a realization of these M random variables drawn from their joint distribution specific to timepoint t_i . From this perspective, the symptom progression matrix describes how the severities of the M symptoms co-evolve over time. To make an interpretable prediction, we need to detect whether such a matrix resembles typical depression or non-depression symptom progression trends such as in Figure 2, which we define as trend prototypes in this study. In the next section, we introduce the computation of trend prototypes.

4.2. Detecting Prototypical Depression Symptom Progression Trends

We first present a conceptual overview of our definition of trend prototype and then discuss the technical details in the subsections. We aim to learn $2K$ trend prototypes: K for the depression category and the remaining K for the non-depression category. We view each trend prototype as a prototypical continuous co-evolution trajectory of the M symptom severities over time, such as trending up, trending down, and fluctuating. Therefore, a trend prototype can be defined as a continuous vector-valued function of time. Let $\mathcal{G}^{(k)}(t)$ denote the k th trend prototype, which maps a time scalar to a vector of symptom severities of length M . The mathematical details of $\mathcal{G}^{(k)}(t)$ will be given in Section 4.2.1. We offer a particular interpretation of trend prototypes: if the focal patient’s symptom progression matrix S strongly resembles trend prototype k , then the symptom severities S_i detected at timepoint t_i should be close to $\mathcal{G}^{(k)}(t_i)$.⁴ Based on this interpretation, the existing strength of trend prototype k in symptom progression matrix S can be measured as the overall closeness between S_i and $\mathcal{G}^{(k)}(t_i)$ over observation timepoints $\langle t_1, t_2, \dots, t_N \rangle$. The implementation of this is articulated in Section 4.2.2.

⁴We use the word “close” rather than “identical” for the definition of trend prototype because the symptom progression matrix of a particular patient is likely to exhibit some idiosyncratic progression patterns that are not common enough to be regarded as prototypical, and therefore S_i is likely to randomly deviate from $\mathcal{G}^{(k)}(t_i)$ by a small amount.

4.2.1. The Definition of Trend Prototypes: A trend prototype is a continuous function of time that characterizes the evolution of symptom severities. This goal necessitates a continuous function that can trace any freely-valued trajectory over time. Studies have shown that any trajectory over time can be decomposed into a summation of sine and cosine curves in the frequency domain (Xu et al. 2020a, Wang et al. 2021a). Inspired by those works, we design the trend prototype as follows. Let $\mathcal{G}_m^{(k)}(t)$ denote the severity of symptom m at timepoint t given by trend prototype k . Leveraging the time encoding method in Xu et al. (2020a), we compute $\mathcal{G}_m^{(k)}(t)$ as

$$\begin{aligned}\mathcal{G}_m^{(k)}(t) &= \sigma\left(\sqrt{\frac{1}{n_d}} \sum_{j=1}^{n_d} p_{k,m,j}^{\mathbb{T}} \cos(\omega_j t + \theta_j) + \sqrt{\frac{1}{n_d}} \sum_{j=1}^{n_d} p_{k,m,n_d+j}^{\mathbb{T}} \sin(\omega_j t + \theta_j)\right) \\ &= \sigma(\Phi(t)^T p_{k,m}^{\mathbb{T}})\end{aligned}\quad (4)$$

where $p_{k,m}^{\mathbb{T}} = [p_{k,m,1}^{\mathbb{T}}, p_{k,m,2}^{\mathbb{T}}, \dots, p_{k,m,2n_d}^{\mathbb{T}}]^T \in R^{2n_d}$ is the coefficient vector specific to trend prototype k and symptom prototype m , $\Phi(t)$ is the time encoding function (Xu et al. 2020a) that transforms timepoint t from a scalar to a numeric vector, defined as

$$\begin{aligned}\Phi(t) &= \sqrt{\frac{1}{n_d}} \left[\cos(\omega_1 t + \theta_1), \cos(\omega_2 t + \theta_2), \dots, \cos(\omega_{n_d} t + \theta_{n_d}), \right. \\ &\quad \left. \sin(\omega_1 t + \theta_1), \sin(\omega_2 t + \theta_2), \dots, \sin(\omega_{n_d} t + \theta_{n_d}) \right]^T\end{aligned}\quad (5)$$

which is parameterized by frequency vector $\omega = [\omega_1, \omega_2, \dots, \omega_{n_d}]$ as well as phase vector $\theta = [\theta_1, \theta_2, \dots, \theta_{n_d}]$, and lastly $\sigma(\cdot)$ is the sigmoid function defined as $\sigma(x) = 1/(1 + \exp(-x))$ to ensure $0 < \mathcal{G}_m^{(k)}(t) < 1$ such that $\mathcal{G}_m^{(k)}(t)$ and $s_{m,i}^{\mathbb{S}}$ are in the same range and therefore comparable to each other. Let $\sigma^{-1}(\cdot)$ denote the inverse of the sigmoid function. Namely, $\sigma^{-1}(x) = \log \frac{x}{1-x}$.

Our design of $\Phi(t)$ ensures that $\sigma^{-1}(\mathcal{G}_m^{(k)}(t))$ is able to trace a freely-valued trajectory over time so that the trajectory of symptom severities can be seamlessly modeled by a continuous function. By learning the three vectors $p_{k,m}^{\mathbb{T}}$, ω and θ as model parameters, while treating n_d as a hyperparameter, Equation 4 amounts to learning a prototypical temporal progression of symptom m in the frequency domain. In a compact form, trend prototype k can be written as

$$\mathcal{G}^{(k)}(t) = \sigma(p_k^{\mathbb{T}} \Phi(t))\quad (6)$$

where $p_k^{\mathbb{T}} \in R^{M \times 2n_d}$ is the coefficient matrix that specifies the function representation of trend prototype k , and is obtained by row stacking the transpose of vectors $p_{k,m}^{\mathbb{T}}$ for $m = 1, 2, \dots, M$. We can view $p_k^{\mathbb{T}}$ as the embedding form of trend prototype k that is analogous to $p_m^{\mathbb{S}}$, the embedding form of symptom prototype m .

Figure 4 shows a few examples of potential depression and non-depression trend prototypes. The depression trend prototypes could be characterized by a rising symptom severity (upper left). Such a severity may have deviations from time to time while keeping the upward trend (upper right).

These trend prototypes correspond to the onset and acute phases in Figure 2. The non-depression trend prototype may be characterized by a downward severity trend (lower left), suggesting a previously depressed patient is recovering. The non-depression trend prototype could also be a curve fluctuating around a fixed level (lower right), indicating the patient never had depression symptoms or has fully recovered from prior depression. When a non-depressed patient relapses, depression trend prototypes, such as the upper two, could reappear in his or her walking sensor data.

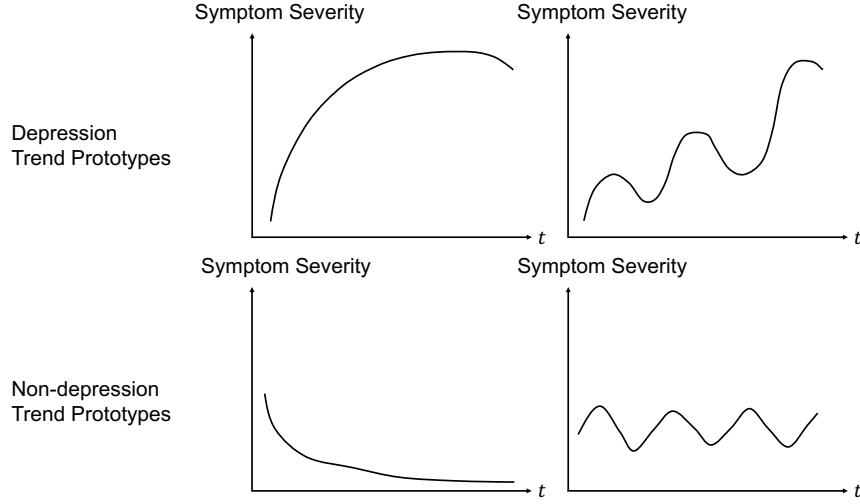


Figure 4 Examples of Trend Prototype

In the subsequent discussion, we will frequently use $\sigma^{-1}(\mathcal{G}^{(k)}(t))$, which means applying the inverse of the sigmoid function element-wisely on $\mathcal{G}^{(k)}(t)$. Therefore, we formally define

$$\tilde{\mathcal{G}}^{(k)}(t) = \sigma^{-1}(\mathcal{G}^{(k)}(t)) = p_k^{\top} \Phi(t) \quad (7)$$

to simplify the notation.

4.2.2. Detecting the Existing Strength of a Trend Prototype: Let s_k^{\top} denote the existing strength of trend prototype k in symptom progression matrix S . Intuitively, s_k^{\top} should be derived by comparing S_i and $\mathcal{G}^{(k)}(t_i)$ for each timepoint t_i , where the former is the “observed” symptom severities detected at t_i , the latter is its corresponding “ideal” values in the prototypical progression patterns captured by trend prototype k . The larger the former deviates from the latter across time, the less likely trend prototype k exists in the symptom progression matrix. However, we argue that for interpretability concerns, S_i should be compared to $\mathcal{G}^{(k)}(t_i - t_0^{(k)})$ rather than $\mathcal{G}^{(k)}(t_i)$, where $t_0^{(k)}$ is a latent variable indicating when the trend starts in the patient’s timeline. The computation and rationale of $t_0^{(k)}$ are articulated below.

Recall that Equation 4 defines $\mathcal{G}^{(k)}(t)$ as a function on the domain $t \in (-\infty, +\infty)$. However, to understand what temporal progression trend prototype k captures, it is necessary to ensure that only a finite segment of $\mathcal{G}^{(k)}(t)$ carries useful information, so that only this segment needs to be visualized to inspect trend prototype k . For this purpose, we need to “bound” the trend by a starting time and an ending time. We treat $t = 0$ as the starting time of trend prototype k , and only work with the right part of $\mathcal{G}^{(k)}(t)$ defined on the non-negative domain $t \in [0, +\infty)$, as shown in Figure 5. This design has two implications. Continuing with the example in Figure 5, on one hand, $\mathcal{G}^{(k)}(0)$ should be treated as the initial state of trend prototype k , and it is the relative timepoint measuring how much time has elapsed since $t = 0$ that truly matters. On the other hand, we can only observe the absolute timepoints when the focal patient performs walking tests in reality (e.g., t_1, t_2 , and t_3). In general, we cannot assume that t_1 , the absolute timepoint of the first walking test performed by the patient, is the starting time of trend prototype k in the patient’s timeline, because t_1 is determined by when the first walking test is performed as well as the range of the observation window. However, the depression progression trend of a patient $\mathcal{G}^{(k)}(t)$ would start regardless of whether a walking test is performed or not. That unobserved trend starting time is noted as $t_0^{(k)}$. If we were able to observe the zero-th walking test X_0 at absolute timepoint $t_0^{(k)}$, and detect symptom severities S_0 from it by computing $s_{m,0}^S$ in accordance with Equation 2 for $m = 1, 2, \dots, M$, then S_0 should be compared to $\mathcal{G}^{(k)}(0)$. In this sense, S_i , the symptom severity vector detected at t_i in the patient’s timeline, should be compared to $\mathcal{G}^{(k)}(t_i - t_0^{(k)})$, the corresponding prototypical values in the trend’s timeline. In Figure 5, the detected symptom severity is compared with trend prototype k by aligning the two timelines at a latent personalized trend starting time $t_0^{(k)}$.

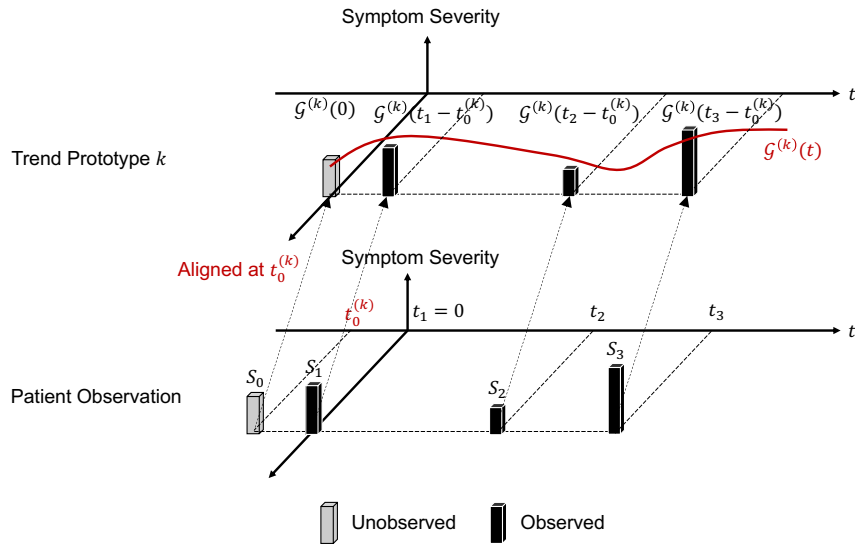


Figure 5 Latent Trend Starting Time

With $t_0^{(k)}$ at hand, only relative timepoints given by $t_i - t_0^{(k)}$ for $i = 1, 2, \dots, N$ carry information. As a result, we set $t_1 = 0$ and measure other timepoints including $t_0^{(k)}$ relative to t_1 without loss of generality. To facilitate the learning of interpretable trend prototypes, we additionally impose the constraint $t_0^{(k)} < t_1 = 0$. If $t_0^{(k)} > 0$, the symptom severities detected before $t_0^{(k)}$ need to be compared to the left part of $\mathcal{G}^{(k)}(t)$ defined on domain $t \in (-\infty, 0)$, which we intend to avoid for interpretability concerns. For example, it is undesired to compare S_1 with $\mathcal{G}^{(k)}(t_1 - t_0^{(k)}) = \mathcal{G}^{(k)}(-t_0^{(k)})$. Allowing such a comparison is in conflict with our interpretation of $t = 0$ as the starting time of trend prototype k . Moreover, it also renders the learned function $\mathcal{G}^{(k)}(t)$ hard to inspect, because the progression patterns within the interval $t \in (-t_0^{(k)}, 0)$ also encode some prototypical patterns summarized from data. Given that $t_0^{(k)}$ varies across patients, the meaningful part of $\mathcal{G}^{(k)}(t)$ is different for different patients. In contrast, if we enforce $t_0^{(k)} < 0$, all detected symptom severities will be compared to the right part of $\mathcal{G}^{(k)}(t)$ defined on the domain $t \in (0, +\infty)$, making $t = 0$ a natural patient-independent starting point to inspect $\mathcal{G}^{(k)}(t)$. Armed with the notion of $t_0^{(k)}$, we proceed to the definition of $s_k^{\mathbb{T}}$ by assuming a pre-computed $t_0^{(k)}$, and then discuss how to infer $t_0^{(k)}$ by the end of this section, where we introduce another design to impose an effective trend ending time.

As pointed out by [Chen et al. \(2019\)](#), a prototype can be viewed as a cluster, and its existing strength in an instance is essentially a closeness measurement between the instance and the cluster. To develop a principled definition of $s_k^{\mathbb{T}}$, we draw inspiration from the Gaussian Mixture Model ([Murphy 2022](#)), a classic clustering algorithm, which measures the closeness between an instance and a cluster in terms of how likely the instance can be generated by the Gaussian component characterized by the cluster. By making an analogy in our context, we view the columns of S as being generated from a time-varying distribution characterized by trend prototype k at aligned timepoints $t_i - t_0^{(k)}$ for $i = 1, 2, \dots, N$. Different from the Gaussian Mixture Model which deals with instances described by freely-valued vectors, the entries of S are bounded in the interval $(0, 1)$. To properly specify the generation of the columns of S , we leverage the logistic-normal distribution, whose samples fall between $(0, 1)$. We introduce this distribution first.

Let $x \sim \mathcal{N}(\mu, \Sigma)$ denote a random vector drawn from the M -dimensional normal distribution of mean $\mu \in R^M$ and covariance $\Sigma \in R^{M \times M}$. Let $z = \sigma(x)$, which is obtained by transforming x element-wisely with the sigmoid function such that $0 < z_m = \sigma(x_m) < 1$ for $m = 1, 2, \dots, M$. Then, z follows $\mathcal{LN}(\mu, \Sigma)$, the M -dimensional logistic-normal distribution with mean μ and covariance Σ , and its density can be computed as

$$\mathcal{LN}(z|\mu, \Sigma) = \frac{1}{\prod_{m=1}^M z_m(1-z_m)} \frac{\exp\left(-\frac{1}{2}(\sigma^{-1}(z) - \mu)^T \Sigma^{-1}(\sigma^{-1}(z) - \mu)\right)}{\sqrt{(2\pi)^M \det[\Sigma]}} \quad (8)$$

where $\sigma^{-1}(z)$ means applying the inverse of the sigmoid function element-wisely on z , and $\det[\Sigma]$ is the determinant of matrix Σ . The derivation of Equation 8 can be found in [Appendix C](#).

Now, consider a focal patient whose symptom progression matrix exhibits the presence of trend prototype k to some extent. In this case, we regard S_i as a realization drawn from the contemporaneous distribution of symptom severities given by $\mathcal{LN}(\tilde{\mathcal{G}}^{(k)}(t_i - t_0^{(k)}), I)$, the M -dimensional logistic-normal distribution characterized by mean $\tilde{\mathcal{G}}^{(k)}(t_i - t_0^{(k)})$ and covariance I (the identity matrix), where $\tilde{\mathcal{G}}^{(k)}(t)$ is defined by Equation 7, and $t_0^{(k)}$ is the personalized trend starting time explained previously. In our setting, S_i is compared to $\mathcal{G}^{(k)}(t_i - t_0^{(k)})$ at the aligned timepoint $t_i - t_0^{(k)}$, while $\tilde{\mathcal{G}}^{(k)}(t)$ depicts the mean series of a time-varying logistic-normal distribution which characterizes some prototypical symptom progression patterns subject to a sigmoid transformation. We assume that the covariance of this time-varying distribution is the constant identity matrix for parsimonious concerns.

The generative process of the symptom progression matrix is summarized in Algorithm 1. Then,

Algorithm 1 The Generative Process of S Characterized by Trend Prototype k

- 1: Compute $t_0^{(k)}$ via Equation 10.
 - 2: Compute $t_i^{(k)} = t_i - t_0^{(k)}$ for $i = 1, 2, \dots, N$.
 - 3: Compute $\tilde{\mathcal{G}}^{(k)}(t_i^{(k)})$ for $i = 1, 2, \dots, N$ using Equation 7.
 - 4: Draw $S_i \sim \mathcal{LN}(\tilde{\mathcal{G}}^{(k)}(t_i^{(k)}), I)$ for $i = 1, 2, \dots, N$.
-

we define $s_k^\mathbb{T}$ as a scalar proportional to the log-likelihood of generating the column vectors of S in accordance with Algorithm 1. Specifically,

$$\begin{aligned}
 s_k^\mathbb{T} &= \sigma \left(\log \prod_{i=1}^N \mathcal{LN}(S_i | \tilde{\mathcal{G}}^{(k)}(t_i^{(k)}), I) \right) \\
 &= \sigma \left(\sum_{i=1}^N \sum_{m=1}^M \log \frac{1}{S_{m,i}(1 - S_{m,i})} - \frac{NM}{2} \log 2\pi - \frac{1}{2} \sum_{i=1}^N \|\sigma^{-1}(S_i) - \tilde{\mathcal{G}}^{(k)}(t_i^{(k)})\|_2^2 \right)
 \end{aligned} \tag{9}$$

where $S_{m,i}$ is the entry at row m and column i in matrix S . The second step of Equation 9 is derived by expanding $\mathcal{LN}(S_i | \tilde{\mathcal{G}}^{(k)}(t_i^{(k)}), I)$ using Equation 8 and then simplifying the resulting terms. The intuition is that the more likely the columns of S can be observed from the generative process characterized by $\mathcal{G}^{(k)}(t)$, the stronger the evidence is that trend prototype k exists in the symptom progression matrix of the focal patient. Equation 9 ensures $0 < s_k^\mathbb{T} < 1$, which means that the existence strength of trend prototypes has the same value range with symptom prototypes as defined by Equation 2. Indeed, by comparing Equations 9 and 2, an obvious analogy can be established between the definition of $s_k^\mathbb{T}$ and $s_{o|m,i}^\mathbb{S}$.

Lastly, we complete the definition of $s_k^\mathbb{T}$ by specifying the inference procedure of $t_0^{(k)}$. Because $t_0^{(k)}$ is used to generate the symptom progression matrix S , given S , we should be able to inversely infer

$t_0^{(k)}$. Based on this intuition, we introduce an inference network, that takes S and the observation timepoints $\langle t_1, t_2, \dots, t_N \rangle$ as input, and outputs $t_0^{(k)}$ as a negative scalar. Specifically, the inference network is defined as

$$h_i^{\mathbb{T}} = \text{GRU}(h_{i-1}^{\mathbb{T}}, S_i \oplus \Phi(t_i)) \quad (10a)$$

$$t_0^{(k)} = -n_w \sigma(w_k^T h_N^{\mathbb{T}}) \quad (10b)$$

In Equation 10a, \oplus is the concatenation operator, $\Phi(\cdot)$ is the time encoding function defined by Equation 5 but parameterized separately, GRU is a Gated Recurrent Unit layer (Cho et al. 2014) used to capture the temporal information in the symptom progression matrix augmented by time features, and lastly $h_i^{\mathbb{T}} \in R^{n_e}$ is the hidden state of the GRU layer at step i . In Equation 10b, $h_N^{\mathbb{T}}$ is the last hidden state of the GRU layer, which serves as a feature vector summarizing the information contained in S and $\langle t_1, t_2, \dots, t_N \rangle$, $w_k \in R^{n_e}$ is a learnable parameter specific to trend prototype k , and $n_w > 0$ is a hyperparameter. Equation 10 enforces that $-n_w < t_0^{(k)} < 0$. We impose this constraint to make the learned trend prototype easier to interpret. Consider the case where the observation window is 2 weeks, which means that the time difference between the first and the last walking test is at most 2 weeks. If we set $n_w = 1$ (time is measured in weeks), then $t_0^{(k)}$ is at most 1 week before the first walking test, which implies that the symptom severities detected from the last walking test will be compared to $\mathcal{G}^{(k)}(3)$ in the most extreme scenario. Consequently, we only need to inspect the segment of $\mathcal{G}^k(t)$ defined on the interval $t \in [0, 3]$, since only this segment has been compared to some real data. In this sense, n_w reflects our belief on which segment of $\mathcal{G}^k(t)$ can be learned from data with reasonable qualities. For example, it should be hard to believe that we could learn a high-quality trend prototype spanning 7 weeks from an observation window lasting only 2 weeks.

4.2.3. Superior Properties of the Trend Prototype: First, no matter how irregularly the focal patient has performed walking tests over time, the symptom progression matrix detected from these walking tests can always be compared to each trend prototype in a consistent manner. The irregularity of inter-test time intervals is explicitly considered, because each trend prototype is a continuous function of time, and therefore the differences in inter-test time intervals are reflected in the evaluation differences of function values. Second, while trend prototype k is learned from irregularly spaced point observations of symptom severities, it can be inspected as a complete temporal symptom progression by evaluating $\mathcal{G}^{(k)}(t)$ at regularly and densely spaced timepoints. Moreover, a trend prototype does not need to be attached to a single patient. Instead, walking test sequences gathered for different patients could be used to learn different segments of a trend prototype, which together pinpoint a complete temporal symptom progression spanning the entire observation window.

4.3. Learning Objective

The classification layer of TempPNet computes the probability of depression given the input sensor signal X of a focal patient, which is defined as

$$P(y = 1|X) = \sigma\left(\sum_{k \in \mathcal{K}^+} s_k^\top - \sum_{k \in \mathcal{K}^-} s_k^\top\right) \quad (11)$$

where $\mathcal{K}^+ = \{1, 2, \dots, K\}$, $\mathcal{K}^- = \{K + 1, K + 2, \dots, 2K\}$, and s_k^\top is defined by Equation 9. The above definition imposes the relationship that a high probability of depression is due to the detection of strong overall existing strength of depression trend prototypes, while weak overall existing strength of non-depression trend prototypes.

The objective function of TempPNet to be minimized is defined based on the binary cross-entropy loss with two additional regularization terms. Specifically,

$$\mathcal{L}_{\text{TempPNet}} = -\frac{1}{|\mathcal{U}|} \sum_{u \in \mathcal{U}} \log P(y^{(u)}|X^{(u)}) + \lambda_{\mathbb{S}} R_{\mathbb{S}} + \lambda_{\mathbb{T}} R_{\mathbb{T}} \quad (12)$$

where $P(y^{(u)}|X^{(u)})$ is computed in accordance with Equation 11 for patient u , $R_{\mathbb{S}}$ and $R_{\mathbb{T}}$ respectively denote the regularization term for the symptom prototypes and the trend prototypes, and lastly, $\lambda_{\mathbb{S}}$ and $\lambda_{\mathbb{T}}$ are the hyperparameters balancing the influence of the regularization terms. Let \mathcal{U}^+ denote the set of depressed patients, and \mathcal{U}^- the set of non-depressed patients. For symptom prototypes, we define $R_{\mathbb{S}}$ as

$$R_{\mathbb{S}} = \frac{1}{M} \sum_{m=1}^M \left(\frac{1}{|\mathcal{U}^-|} \sum_{u \in \mathcal{U}^-} \frac{1}{N_u} \sum_{i=1}^{N_u} s_{m,i|u}^{\mathbb{S}} - \frac{1}{|\mathcal{U}^+|} \sum_{u \in \mathcal{U}^+} \frac{1}{N_u} \sum_{i=1}^{N_u} s_{m,i|u}^{\mathbb{S}} \right) \quad (13)$$

where $s_{m,i|u}^{\mathbb{S}}$ is the symptom severity computed in accordance with Equation 2 for patient u , and $\frac{1}{N_u} \sum_{i=1}^{N_u} s_{m,i|u}^{\mathbb{S}}$ is the average severity level of symptom m detected in the walking test sequence of patient u . Minimizing $R_{\mathbb{S}}$ enforces that the average symptom severity level should be on average higher in the depressed group than it is in the non-depressed group for all symptoms, and thereby imposes our expected interpretation of symptom prototypes. For trend prototypes, we define $R_{\mathbb{T}}$ as

$$R_{\mathbb{T}} = \frac{1}{|\mathcal{U}^+|} \sum_{u \in \mathcal{U}^+} \left(\max_{k \in \mathcal{K}^-} s_{k|u}^{\mathbb{T}} - \min_{k \in \mathcal{K}^+} s_{k|u}^{\mathbb{T}} \right) + \frac{1}{|\mathcal{U}^-|} \sum_{u \in \mathcal{U}^-} \left(\max_{k \in \mathcal{K}^+} s_{k|u}^{\mathbb{T}} - \min_{k \in \mathcal{K}^-} s_{k|u}^{\mathbb{T}} \right) \quad (14)$$

where $s_{k|u}^{\mathbb{T}}$ is the trend existing strength computed in accordance with Equation 9 for patient u . Minimizing the first (second) summation term in Equation 14 encourages the model to detect strong existing evidence for at least one depression (non-depression) trend prototype from the walking test sequence of each depressed (non-depressed) patient, while weak existing evidence for all non-depression (depression) trend prototypes from the same walking test sequence.

4.4. Prototype Visualization

TempPNet interprets its prediction according to the following mechanism. If the focal patient is classified into the depression class, we must have $P(y = 1|X) > 0.5$ under the decision threshold 0.5, which implies that $\sum_{k \in \mathcal{K}^+} s_k^\top > \sum_{k \in \mathcal{K}^-} s_k^\top$, i.e., the overall existing strength of depression trend prototypes must be stronger than non-depression trend prototypes. In this case, we can interpret the prediction made by TempPNet by inspecting the depression trend prototypes that strongly present in the walking test sequence of the focal patient, i.e., trend prototypes with values of s_k^\top . Different from existing prototype learning methods, where prototypes are learned in a latent space that is not directly interpretable (Chen et al. 2019), the trend prototypes learned by TempPNet can be directly inspected by visualizing them as trajectories of symptom severities evolving over time, as illustrated by Figure 4. Moreover, as explained in Section 4.2.2, to inspect one trajectory of a trend prototype, it is enough to visualize its segment for the time interval $t \in [0, n_w + n_T]$, where n_w is the hyperparameter defined in Equation 10b, and n_T is the observation window defined as the maximum span from the timepoint of the first walking test to the timepoint of the depression label. In this study, we measure time t in days, and set n_w as 5 days, while n_T as 14 days.

However, trend prototype $p_{k,m}^\top$ does not stand alone. It depicts the typical temporal progression pattern of symptom m . Therefore, visualizing the underlying symptom prototype m is critical for a thorough understanding of model decisions. Given that the learned embedding vector of symptom prototype m is $p_m^\mathbb{S}$, we leverage the sensor data to offer an interpretation for $p_m^\mathbb{S}$ in the following approach. First, we search for the particular walking test where symptom prototype m presents most strongly across all patients. Mathematically, this means solving for the combination $(u^*, i^*) = \arg \max_{u,i} s_{m,i|u}^\mathbb{S}$ where $u \in \mathcal{U}$ and $i \in \{1, 2, \dots, N_u\}$. Second, based on the identified sensor signal sequence $X_{i^*}^{(u^*)}$, we use Equation 2 to further search for the particular patch o^* where symptom prototype m presents most strongly. Mathematically, $o^* = \arg \max_o s_{o|m,i^*}^\mathbb{S}$ where $o \in \{1, 2, \dots, n_o\}$ and the patient index u^* is omitted for simplicity. Lastly, we inspect symptom prototype m by visualizing the receptive field of this patch, which corresponds to a local segment in $X_{i^*}^{(u^*)}$ that contributes mostly to the computation of $H_{o^*|i^*}^\mathbb{S}$, the embedding vector of this patch defined by Equation 1. To this end, we adopt the gradient-based approach (Luo et al. 2016). For each timepoint l in $X_{i^*}^{(u^*)}$, we compute $\partial H_{o^*|i^*}^\mathbb{S} / \partial a_l$, which is the Jacobian matrix of the patch embedding vector w.r.t. the sensor feature recorded at timepoint l . By measuring the overall importance score of a_l relative to $H_{o^*|i^*}^\mathbb{S}$ as $\|\partial H_{o^*|i^*}^\mathbb{S} / \partial a_l\|$, the Frobenius norm of the Jacobian matrix, we can pinpoint the receptive field of patch o^* as a local segment in $X_{i^*}^{(u^*)}$ within which the importance scores of sensor signal inputs are above a pre-specified threshold such as zero.

5. Empirical Analyses

5.1. Data Collection and Preprocessing

We obtained the mPower dataset, a smartphone-based study that collects daily motion sensor signals for chronic disease patients (Bot et al. 2016). To acquire the depression label, we leverage the MDS-UPDRS survey from this dataset. The MDS-UPDRS survey is originally used to evaluate Parkinson’s disease severity. Part of its questions overlaps with the PHQ-9 depression assessment questionnaire. We select those overlapped questions to measure depression status, including MDS-UPD 1.1, 1.3-1.5, and 1.7-1.8, whose total score is 24. In clinical practice, patients with a PHQ-9 score over 4 (total score is 27) are diagnosed as depressed (Patient 2022). Similarly, we label patients whose MDS-UPD score is over $24 \times 4/27 \approx 3$ as depressed and the remaining as non-depressed.

To construct our input data, we utilize the accelerometer and gyroscope data from the mPower dataset. These data are collected from walking tests – each test is composed of walking 20 steps in a straight line (outbound), turning around and standing for 30 seconds (rest), and walking 20 steps back (return). In the walking tests, the accelerometer records a tri-axial acceleration reading $[x_a^g, y_a^g, z_a^g]$, and the gyroscope records a four-dimensional rotation and orientation reading $[x_o, y_o, z_o, w_o]$. Both readings are sampled at a frequency of 100 Hz. To reduce noise and prevent overfitting, we follow the standard sensor data preprocessing technique (Sigcha et al. 2020) to resample the readings at a frequency of 10 Hz. For each patient, we select a window of two weeks before they took the MDS-UPDRS survey and utilize the accelerometer and gyroscope data in this time window as the sensor input for this patient. The two-week time window is used in clinical practice to diagnose depression, such as the PHQ-9 questionnaire. In the end, we generated a dataset of 3,154 walking tests, encompassing 916 chronic disease patients (496 depressed and 420 non-depressed). Each walking test includes a sequence of motion sensor readings. Due to the complexity and high budget of sensor data collection, our data size is in line with or larger than most sensor-based disease prediction studies (Zhu et al. 2021, Jacobson and Chung 2020, Farhan et al. 2016, Moon et al. 2020, Coelln et al. 2019). We split this dataset into 60% for training, 20% for validation, and 20% for test.

5.2. Benchmark Methods

According to our literature review, we select three groups of benchmarks. The first group includes the state-of-the-art and the most widely recognized interpretable prototype learning methods, ProtoPNet (Chen et al. 2019) and ProSeNet (Ming et al. 2019). These are the most related benchmarks to this study. Compared to our model, these benchmarks cannot model or interpret the temporal symptom progression. The second group is black-box deep learning models, CNN and RNN. They have been commonly used in prior motion sensor-based predictions (Yu et al. 2022, Zhu et al. 2021). The third group uses manually crafted features, such as mean and variance, as the input

(Oung et al. 2015, Yu et al. 2022). These features are reported in Appendix D. The benchmarks in the third group are in line with Yu et al. (2022), which includes k-nearest neighbors (KNN), support vector machine (SVM), random forest, AdaBoost, and XGBoost. The hyperparameters of the benchmarks are summarized in Table 4. These hyperparameters are fine-tuned for each benchmark after large-scale experiments. The following evaluation results report the fine-tuned performances for the benchmarks.

Table 4 Benchmark Hyperparameter Settings

Model	Parameter	Values
TempPNet	CNN channels	(256, 512, 256, 128)
	CNN kernel sizes	8×1
	Time encoding dimensions	64
ProtoPNet	CNN channels	(32, 64, 128, 256)
	CNN kernel sizes	3×3
ProSeNet	GRU hidden units	64
KNN	Number of neighbors	5
SVM	Regularization parameter	1
	Kernel coefficient	0.001
Random Forest	Number of estimators	100
AdaBoost	Number of estimators	50
XGBoost	Number of estimators	100
	Minimum loss reduction for further partition	1.5
	Subsample	0.6

To implement our model, we adopt the following hyperparameter setting. We set the embedding dimension of symptom prototypes as $n_e = 128$, the time embedding dimension as $n_d = 64$, the regularization weights as $\lambda_S = 0.1$ and $\lambda_T = 0.1$. For the specification of the CNN layer, please refer to Appendix B. We train our model with the Adam optimizer (Kingma and Ba 2015) with a learning rate of 0.001 and a batch size of 32.

5.3. Depression Prediction Evaluation

We adopt F1-score, precision, and recall as the evaluation metrics. The best model should have the highest F1-score. The prediction performance, input, and interpretability of our model and the benchmarks are reported in Table 5. These performances are the mean of 10 experimental runs. For the deep learning-based models, we also report the standard deviation of the performances.

Compared to the best-performing prototype learning model (ProSeNet), TempPNet improves F1-score by 0.106. Such a significant performance gain indicates that capturing temporal symptom progression greatly contributes to depression prediction. Compared to the best deep learning model (RNN), our model increases F1-score by 0.097. This increase is attributed to our model’s capability of capturing temporal symptom progression and depression symptoms. Compared to the

Table 5 Prediction Performance Evaluation

Model	Input	Interpretable	F1-score	Precision	Recall
TempPNet (Ours)	Raw sensor	Yes	0.765 ± 0.006	0.737 ± 0.013	0.796 ± 0.013
ProtoPNet	Raw sensor	Yes	0.641 ± 0.018	0.554 ± 0.014	0.761 ± 0.039
ProSeNet	Raw sensor	Yes	0.659 ± 0.024	0.555 ± 0.016	0.814 ± 0.055
CNN	Raw sensor	No	0.655 ± 0.056	0.534 ± 0.012	0.861 ± 0.151
RNN	Raw sensor	No	0.668 ± 0.023	0.544 ± 0.005	0.870 ± 0.083
KNN	Features	No	0.514	0.567	0.469
SVM	Features	No	0.649	0.577	0.741
Random forest	Features	No	0.614	0.600	0.630
AdaBoost	Features	No	0.550	0.557	0.543
XGBoost	Features	No	0.584	0.616	0.556

leading feature-based ML model (SVM), TempPNet boosts F1-score by 0.116. This performance enhancement is due to our model’s ability to learn effective features from the raw sensor signal.

The prediction performance improvement brings prominent economic value. Depression prediction is inherently accompanied with true positive benefits and false positive costs. The true positive benefits are estimated to be the savings from intervening untreated depression, so that depression-induced lost productivity and the healthcare expenditure from related complications can be mitigated. Such intervention can be informed via deploying our method in mobile applications. There are an estimated 307 million smartphone users in the US ([Statista 2022](#)), representing 93.3% of the US’s 329 million population. The annual cost of untreated depression in the US is \$150 billion ([Rampell 2013](#)), among which the mobile users contribute $150 \times 93.3\% = \$139.95$ billion. Assuming all true positive patients detected by our model are treated properly, the benefit of true positive from saving the untreated depression amounts to up to $\$139.95 \times \text{recall}$ (billion).

Beyond improving true positives, minimizing false positives deserves special attention in depression prediction. False positives can cause inconvenience and time and cost of further doctor appointments. Consequently, the falsely identified patients may suffer from stigma ([Martin et al. 2017](#)), and the doctors and hospitals need to shoulder an opportunity cost, whereby time and effort devoted to screening may be more profitably used for other activities. At the system level, inefficient use of resources can result from responding to false positives and over-diagnosis (i.e., treating illness that would have remitted naturally or not led to suffering or impairment) ([Martin et al. 2017](#)). According to [Heslin et al. \(2022\)](#), false positives of depression account for 20% of the resources for treatment. The annual cost of depression treatment in the US is \$326 billion⁵, or $326 \times 93.3\% = \$304$ billion for mobile users. Therefore, the cost of false positive is approximately $\$304 \times 20\% \times (1 - \text{precision})$ (billion). Table 6 shows the economic analysis for the depression prediction.

Compared to the baseline models, the annual net benefit that our model brings (\$95.410) is significantly higher. The leading prediction accuracy of TempPNet, coupled with its tremendous

⁵Depression Cost the US \$326 Billion Per Year Pre-Pandemic, a 38% Increase Since 2010

Table 6 Annualized Economic Benefit Analysis for Prediction (for the US)

Model	Precision	Recall	Benefit for True Positive (Billion)	Cost for False Positive (Billion)	Net Benefit (Billion)
TempPNet (Ours)	0.737	0.796	\$111.400	\$15.990	\$95.410
ProtoPNet	0.554	0.761	\$106.502	\$27.117	\$79.385
ProSeNet	0.555	0.814	\$113.919	\$27.056	\$86.863
CNN	0.534	0.861	\$120.497	\$28.333	\$92.164
RNN	0.544	0.870	\$121.757	\$27.725	\$94.032
KNN	0.567	0.469	\$65.637	\$26.326	\$39.310
SVM	0.577	0.741	\$103.703	\$25.718	\$77.985
Random forest	0.600	0.630	\$88.169	\$24.320	\$63.849
AdaBoost	0.557	0.543	\$75.993	\$26.934	\$49.058
XGBoost	0.616	0.556	\$77.812	\$23.347	\$54.465
No intervention	0	0	\$0	\$0	\$0

economic benefits, proves the validity and societal impact of our model. Even though RNN has a comparable net benefit, this is because its recall is high. However, RNN’s precision is rather low which leads to a high false positive rate. Beyond economic cost, false positive results in many unmeasurable social ramifications, such as mental burden, inconvenience, potential stigma, adverse events of treatment, and mission creep (treating non-illness for security) (Martin et al. 2017). In addition, RNN is a black-box model, which is inferior to interpretable counterparts in healthcare predictions.

Since our model consists of multiple critical design components, we further perform ablation studies to show their effectiveness, as reported in Table 7. We first remove the latent trend starting time design ($t_0^{(k)}$). We also remove the trend prototype design. After removing the trend prototype, the model loses the capability of detecting temporal symptom progression. Consequently, we test two options: using the last symptom severity to predict depression and using the average symptom severity over time to predict depression. Table 7 suggests that removing any design component will significantly hamper the prediction accuracy, proving that our design choice is optimal.

Table 7 Ablation Studies

Model	F1-score	Precision	Recall
TempPNet (Ours)	0.765 ± 0.006	0.737 ± 0.013	0.796 ± 0.013
TempPNet removing offset $t_0^{(k)}$	0.733 ± 0.017	0.624 ± 0.046	0.897 ± 0.060
Remove trend prototype using last symptom severity	0.753 ± 0.023	0.687 ± 0.043	0.836 ± 0.028
Remove trend prototype using average symptom severity	0.733 ± 0.017	0.653 ± 0.043	0.842 ± 0.058

As our model takes the sensor data from an observation window as the input, we analyze how the length of the observation window influences the prediction accuracy. We show the results of the 2-week, 4-week, 8-week, and 16-week observation windows in Table 8. The results indicate a 2-week observation window reaches the best performance. This is also in line with the clinical practice. In

the PHQ-9 depression questionnaire that is used to clinically diagnose depression, the timeframe for mental health observation is two weeks. Beyond two weeks, patients may have depressive and non-depressive episodes from time to time. Thus, noisy observations arise. Therefore, we use the 2-week observation window for all the other analyses.

Table 8 Analysis of Observation Window (Signal Frequency = 10 Hz)

Observation Window	F1-score	Precision	Recall
2 weeks	0.765 ± 0.006	0.737 ± 0.013	0.796 ± 0.013
4 weeks	0.735 ± 0.021	0.639 ± 0.063	0.879 ± 0.064
8 weeks	0.741 ± 0.017	0.670 ± 0.076	0.851 ± 0.091
16 weeks	0.732 ± 0.004	0.664 ± 0.069	0.840 ± 0.107

To reduce noise in the sensor data and avoid overfitting, sensor-based prediction studies usually downsample the sensor signals (Sigcha et al. 2020). We test the effect of different sample rates in Table 9: 10 Hz, 20 Hz, and 30 Hz. The results suggest that 10 Hz signal frequency achieves the best performance. Therefore, we use the 10 Hz signal frequency for all the other analyses.

Table 9 Analysis of Signal Frequency (Observation Window = 2 Weeks)

Signal Frequency	F1-score	Precision	Recall
10 Hz	0.765 ± 0.006	0.737 ± 0.013	0.796 ± 0.013
20 Hz	0.728 ± 0.015	0.603 ± 0.042	0.925 ± 0.054
30 Hz	0.738 ± 0.025	0.620 ± 0.060	0.927 ± 0.057

5.4. Interpretation of Depression Prediction

Beyond depression prediction, TempPNet is capable of interpreting why a patient is classified as depressed by presenting the contributing temporal symptom progression (trend prototype) and the corresponding walking symptom (symptom prototype). Figure 6 shows the most salient trend prototypes that our model learned. For each picture, the x-axis is time, and the y-axis is symptom severity.

Trend prototypes (1)-(5) are depression trend prototypes. They represent the severities of depression symptoms trending up. Some of them have deviations from time to time in the upward trend, such as (2)-(4), representing temporary symptom relief and deterioration of depression. This conforms with the typical depression trend (Bockting et al. 2015). Trend prototypes (6)-(10) are non-depression trend prototypes, where (6), (7), (9), and (10) represent trending down and (8) represents fluctuating with no trend. These are not typical depression trends. Each trend prototype is coupled with underlying symptoms. Figure 7 shows the symptom prototypes that our model learned.

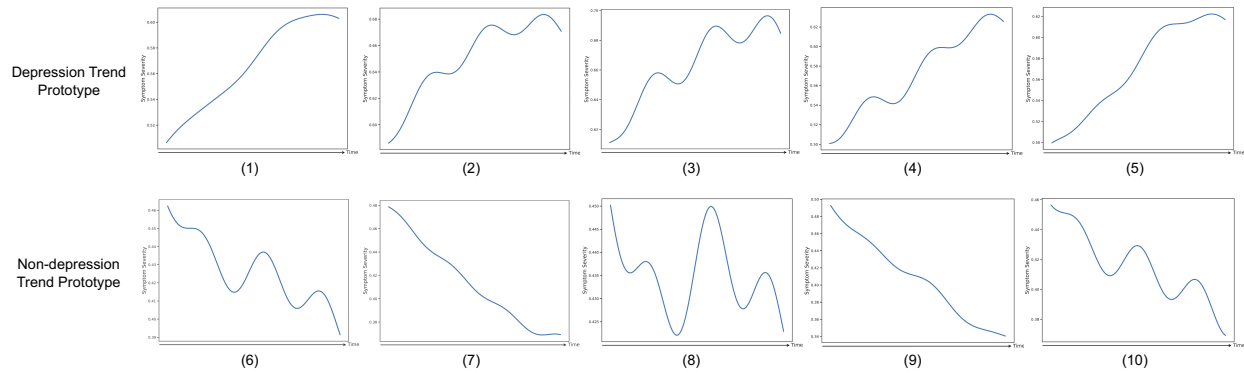


Figure 6 Trend Prototypes

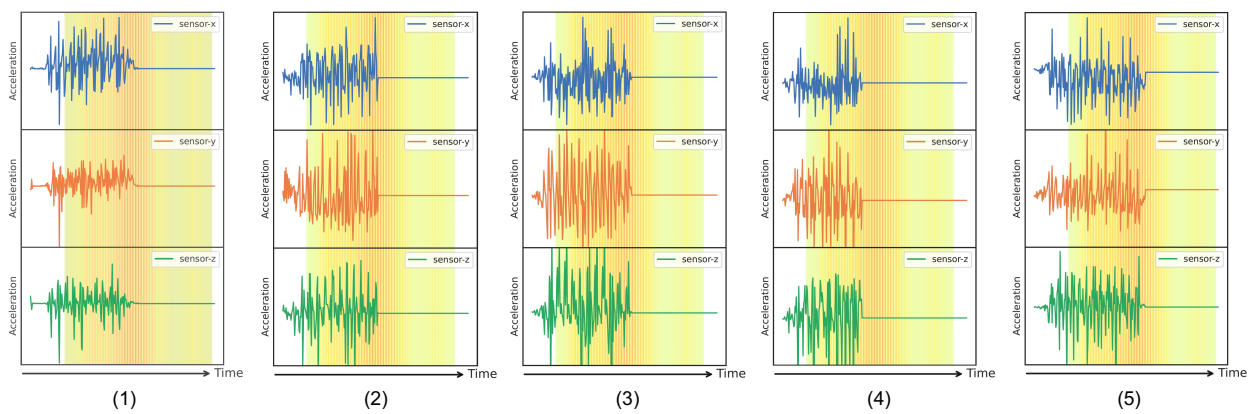


Figure 7 Symptom Prototypes

The prototype visualization in Figure 7 shows the sensor signal of the symptoms. Prior literature suggests that depression walking symptoms can be reflected in gait features, such as walking speed, stride, and speed of the lifting motion of the leg (Sloman et al. 1982, Lemke et al. 2000, NHS 2022). When interpreting the prediction of a patient, these gait features can be computed for the symptom prototypes. The yellow area is the receptive field that presents the corresponding symptom. The darker the color, the stronger the symptom is present in that region.

Leveraging the above-learned trend prototypes and symptom prototypes, our model can interpret the prediction of depression for every patient. We randomly select two patients (one depressed and one non-depressed) and showcase TempPNet’s interpretation for them. Figure 8 shows the interpretation of the depressed patient, and Figure 9 shows the interpretation of the non-depressed patient. For simplicity, we only show the trend prototype with the highest existing strength and the corresponding symptom prototype with the highest existing strength in these examples. For the symptom prototype, we also compute the gait features using the GaitPy package⁶ to explain the encoded information from the visualization.

⁶<https://pypi.org/project/gaitpy/>

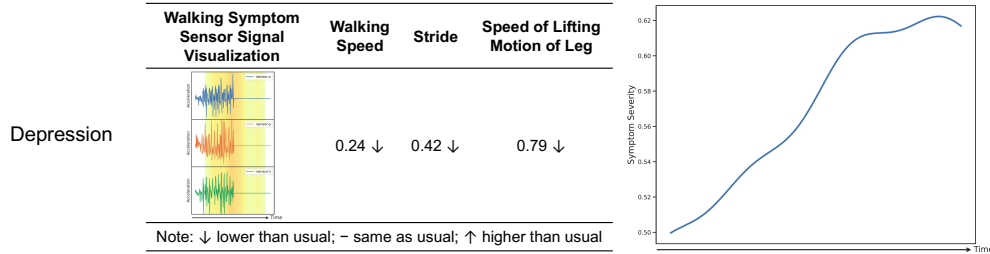


Figure 8 Interpretation of A Depressed Patient

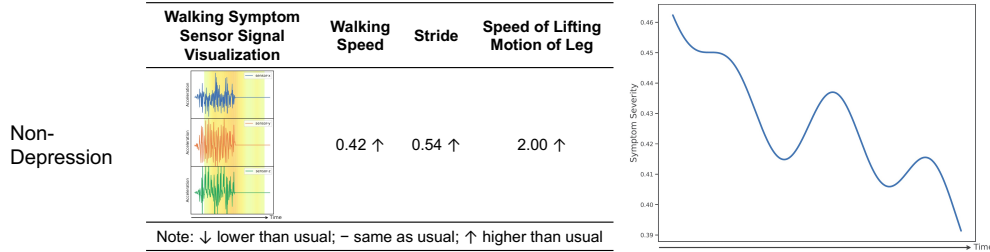


Figure 9 Interpretation of A Non-depressed Patient

TempPNet predicts the patient in Figure 8 as depressed for two reasons. First, this patient’s walking patterns strongly present a walking symptom like in the left part of Figure 8. This walking symptom is manifested as slower-than-usual walking speed⁷, shorter stride, and slower lifting motion of the leg. This symptom conforms with the depression physical symptoms in the literature (Sloman et al. 1982, Lemke et al. 2000, NHS 2022). Second, the severity of the previously mentioned symptom presents a temporal progression pattern like the right part of Figure 8. TempPNet believes this temporal symptom progression pattern resembles a typical depression progression pattern. According to the depression progression literature (Bockting et al. 2015, Dattani et al. 2021), this judgment makes sense — this patient’s depression walking symptom first worsens rapidly and then peaks, similar to the onset and acute phases in Figure 2.

TempPNet predicts the patient in Figure 9 as non-depressed for two reasons. First, this patient’s walking patterns strongly present a walking symptom like in the left part of Figure 9. This walking symptom is manifested as faster-than-usual walking speed, longer stride, and faster lifting motion of the leg. This symptom does not resemble the typical depression walking symptoms in the related literature (Sloman et al. 1982, Lemke et al. 2000, NHS 2022). Second, the severity of the previously mentioned symptom presents a temporal progression pattern like the right part of Figure 9. The symptom severity trends down and has fluctuations in the middle. This trend does not resemble a typical depression trend.

As medical experts are aware of what a typical depression walking pattern may look like (e.g., walking symptoms and temporal symptom progression), our interpretation greatly helps doctors

⁷The usual case is computed as the mean of each gait feature among the non-depressed participants in the dataset.

understand why a patient is predicted as depressed. When our interpretation matches the medical understanding, as is the case in Figures 8 and 9, doctors would trust our model’s prediction much more. Based on our interpretation, doctors can also assess what symptoms the patient presents and in what phase of the depression progression the patient is at. This interpretation information coupled with our prediction result could subsequently inform doctors to take corresponding interventions to treat depression with increased confidence and precision.

5.5. Human Evaluation

The major contribution of TempPNet in interpretation lies in its capability of interpreting temporal symptom progression. To validate that capturing temporal symptom progression actually improves users’ trust in our model, we conduct a user study. We recruited 80 college students and informed the participants that they would be assigned an interpretable ML model to predict depression using sensor data. We randomly selected one patient sample that the model predicted as depressed and show the participants how the model interpreted this prediction. We design two randomized groups: one to present TempPNet’s interpretation, and the other to present the baseline’s interpretation (without temporal symptom progression, which is equivalent to ProtoPNet).

The first part of the user study collects five control variables: age, education, gender, trust in AI, and health literacy. This user study passed randomization checks. The summary statistics and randomization p -values are reported in Tables 10, 11, and 12.

Table 10 Summary Statistics (Categorical)

Variable	Category	Count	Variable	Category	Count
Age	18 and lower	1	Education	College freshman	1
	18-24	28		College sophomore	9
	25-34	23		College junior	3
	35-44	4		College senior	8
	45-54	2		Master	22
	55-64	2		Doctorate	17
Gender	Female	29			
	Male	31			

Table 11 Summary Statistics (Continuous)

Statistics	Min	1st Qu.	Median	Mean	3rd Qu.	Max
Trust in AI	1	3	3	3.2	4	4
Health Literacy	1.250	2.688	3.000	3.033	3.500	4.000

Since the interpretation is based on depression walking symptoms, we designed a depression knowledge education session for all participants. We ask the participants to read the related depression knowledge depicted in Figure 10a. After reading such information, they are asked to answer

Table 12 Randomization Checks

	Age	Education	Gender	Trust in AI	Health Literacy
P-value	0.893	0.195	0.958	0.544	0.788

four questions in Figure 10b to test their understanding. If they answer these questions incorrectly, an error message such as in the top line of Figure 10b will prompt and direct them to read the information and choose again. After they answer the test questions correctly, they have sufficient knowledge to understand the model interpretations.

Read the information about the physical symptoms of depression. Then answer the following questions.

Physical symptoms have been shown to be an essential manifestation of depression:

- Sloman et al. (1982) found that compared to healthy controls, **depressed patients' walks are slower** and the **lifting motion of the leg is slower**.
- Lemka (2020) showed that **depressed patients have shorter strides** and **slower gait velocity** than healthy controls.

(a) Knowledge Training Reading

Incorrect answer. Please read the background knowledge and choose again.

Please pick one group for each question.

	Depressed Patients	Healthy Control
Who usually walk more slowly?	<input checked="" type="radio"/>	<input type="radio"/>
Whose lifting motion of the leg is slower?	<input checked="" type="radio"/>	<input type="radio"/>
Whose strides are longer?	<input type="radio"/>	<input checked="" type="radio"/>
Whose gait velocity is faster?	<input checked="" type="radio"/>	<input type="radio"/>

(b) Knowledge Training Test

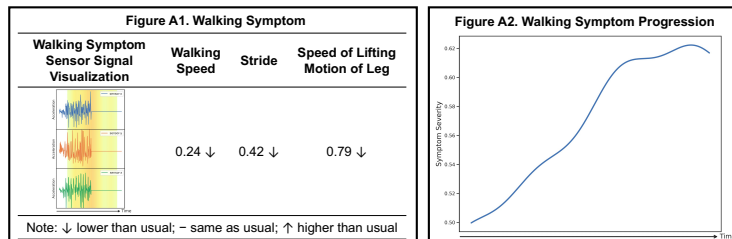
Figure 10 Depression Knowledge Training

In the next part of the user study, we inform the participants the prediction context, input, and output. Then, we show the model interpretation to each group respectively, as shown in Figure 11. The size of the pictures is the same for both groups in the survey. A manipulation check question is asked to verify whether the participants read the interpretation carefully (“How does the walking speed of the above walking symptom compare to the usual case?”), whose answer can be understood from the arrow sign after the value of the walking speed in the interpretation figure. Subsequently, we ask the participants to rate their trust in the given model. The measurement scale is adopted from Chai et al. (2011). The Chronbach’s Alpha is 0.901 for this scale, suggesting excellent reliability. The factor loadings of the scale are reported in Appendix E, suggesting good validity. In this scale, an attention check question is added (“Please just select neither agree nor disagree.”). After removing the participants who failed the attention check or the manipulation check, 60 participants remain in the final analyses. Figure 12 shows the mean of trust for each of the two groups. The participants’ trust in our model (mean = 2.31) is significantly higher than the baseline model (mean = 1.65, $p < 0.001$). This result indicates that interpreting the temporal symptom progression is a critical booster for users’ trust in depression prediction models, endorsing our model design.

Input: walking sensor signals of a patient
Model A's prediction outcome: depressed

Model A's interpretation of this prediction includes two parts:

1. As shown in Figure A1: This patient is predicted as depressed because he/she presents Figure A1's walking symptom, whose sensor signal visualization and walking features are also presented. The walking features are indicated whether they are higher or lower than usual using an arrow sign after the number.
2. As shown in Figure A2: The severity of the walking symptom in Figure A1 also progresses over time like in Figure A2.

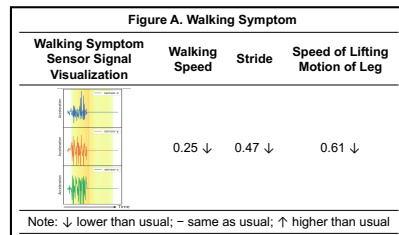


(a) Group TempPNet

Input: walking sensor signals of a patient
Model A's prediction outcome: depressed

Model A's interpretation of this prediction includes one part:

1. As shown in Figure A: This patient is predicted as depressed because he/she presents Figure B's walking symptom, whose sensor signal visualization and walking features are also presented. The walking features are indicated whether they are higher or lower than usual using an arrow sign after the number.



(b) Group Baseline

Figure 11 User Study Groups

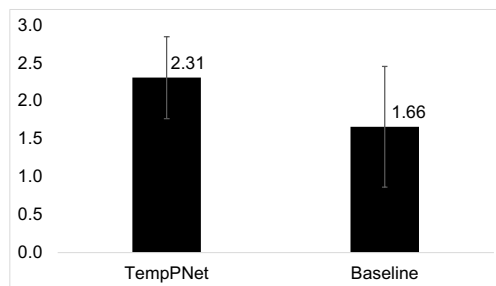


Figure 12 Trust Comparison Between TempPNet and Baseline

After the participants rate the trust for the given model, we then show them the interpretation of the other model as a comparison. We ask them to choose a model interpretation that they trust more. 50 participants (83.3%) chose TempPNet over the baseline. When asked why they trust TempPNet more than the baseline, 31 participants mentioned, in similar wording, that “because this model visualized the walking symptom progression.” The above user study results prove that by interpreting the temporal symptom progression, TempPNet improves users’ trust in our model, which offers empirical evidence for the contribution of our model innovation.

6. Discussion and Conclusions

Depression prediction is fundamental to comprehensive chronic care in the health sensing area. Although a few studies tapped this domain, they do not offer a meaningful interpretation of their predictions. Prototype learning methods, a class of state-of-the-art interpretable methods, fall short in modeling the temporal progression of depression. To address these limitations, we propose a novel interpretable deep learning method to predict depression using sensor data while interpreting

its predictions based on the temporal progression of depression. We conduct extensive evaluations to demonstrate superior predictive power of our method over state-of-the-art benchmarks and showcase its interpretation of predictions. Furthermore, through a user study, we show that our method outperforms these benchmarks in terms of interpretability.

Our study contributes to the extant literature in two aspects. First, our work belongs to the computational genre of design science research, which develops computational methods to solve business and societal problems and aims to make methodological contributions (Rai 2017, Simchi-Levi 2020, Padmanabhan et al. 2022). In this regard, our proposed TempPNet is a novel prototype learning method that processes a sequence of inputs and interprets predictions based on prototypes of temporal symptom progression. To design TempPNet, we innovatively overcome three methodological challenges: learning prototypes of depression symptoms, learning prototypes of temporal symptom progression from walking tests performed at irregular time intervals, and modeling walking tests of varying lengths. Second, our study contributes to healthcare IS research with a novel interpretable deep learning method that predicts depression associated with chronic diseases using motion sensor data and interprets its predictions.

6.1. Research and Practical Implications

This study has implications for predictive and prescriptive analytics research. Over the years, methods that predict future actions (i.e., predictive analytics) or specify optimal decisions (i.e., prescriptive analytics) have been developed to solve problems in a diverse set of domains such as health analytics, video analytics, and social media analytics (Xie and Liu 2020, Yu et al. 2022). Our proposed method is particularly useful for those models that rely on snapshot information to make a prediction but neglect the temporal changes of such information. For example, one closely related area that TempPNet can be generalized to is Parkinson’s disease (PD) progression prediction and interpretation. Similar to our study, motion sensor data can be collected to reflect the motion symptoms of PD. The symptom prototype of our method can detect typical PD walking symptoms, such as smaller steps, slower speed, less trunk movement, and a narrow base of support.⁸ PD patients’ symptoms may also form a trend. The trend prototype of our method is able to detect such a trend, predict PD severity, and interpret such a prediction.

Consider another application area, as sensor data naturally resemble image data, TempPNet can be used to process time-series images, or videos. The applicable tasks include object detection, video classification, among others. The symptom prototype in our method can be adapted to recognize typical objects in each video frame, and the trend prototype can be used to capture the temporal changes of these objects, such as shape and angle changes, location moves, and context

⁸<https://www.parkinson.org/understanding-parkinsons/symptoms/movement-symptoms/trouble-moving>

shifts. Beyond the above-mentioned applications, TempPNet can be generalized to interpretable prediction problems where the temporal progression of information is essential.

Our proposed method holds significant practical implications. For doctors, our method can be deployed in mobile applications. Doctors can encourage their chronic disease patients to install these applications to actively monitor patients' walking data. Our method is able to predict the depression risk on a daily basis. When our method signals a high depression risk, the doctors could review the interpretation given by our model and understand what depression walking symptoms the patient presents and how the patient's depression severity has progressed over time. Timely and personalized interventions can be taken to prevent the deterioration of depression and the negative spill-over effects for physical chronic symptom treatments. For caregivers, our method offers an opportunity to keep track of the daily mental health updates of their loved ones. When the mental health deteriorates, the caregivers can actively seek medical help, provide emotional support, and look for social support groups for the patients. For patients, our method can provide a daily health check dashboard, so that they are aware of their mental health status. For the healthcare system, since depression poses a significant economic burden, our method enables active monitoring of depression and timely intervention, thus greatly reducing the preventable mental illness costs and related complications for the linked main chronic disease treatment.

6.2. Limitations and Future Research

Our study has a few limitations and can be extended in multiple directions. First, our walking signals are collected via walking tests from the mPower study (Bot et al. 2016). Although clinical studies have proven that walking tests are a reliable test for assessing functional symptoms of depressed patients (Vancampfort et al. 2020), continuous collection of sensor signals could provide a richer reflection of depression symptoms. Nevertheless, continuous sensor data collection while matching the scale of the mPower study necessitates significant costs, including mobile application development, recruiting and obtaining consent from participants, and data storage, among others. If budgets permit, future studies can conduct natural experiments to collect continuous sensor data for chronic disease patients and improve the training data of our model. Second, similar to any experimental studies, it is likely that participants may attempt to perform a desired behavior in the walking test that they would not normally do in real life. This issue is mitigated in this study. The mPower study is a longitudinal study with a general purpose of health management for chronic disease patients. Patients are not anchored to change any behavior related to depression. Besides, this study focuses on major depressive disorder which is persistent and has significant impairment (Mayo Clinic 2022), instead of temporary mood swings. Such persistent symptoms are difficult to self-control. Because of that, Vancampfort et al. (2020) have proved that self-conducted walking

tests can reliably reveal the physical symptoms of depression. Even in professional clinical settings, many disorders involving movement impairment, such as Parkinson’s disease, are also diagnosed via walking tests in the doctor’s office (Yu et al. 2022). If research budgets are available, future studies could collect the sensor data continuously without having to initiate the test setting.

References

- Anand S, Stepp CE (2015) Listener Perception of Monopitch, Naturalness, and Intelligibility for Speakers With Parkinson’s Disease. *Journal of Speech, Language, and Hearing Research* 58(4):1134–1144.
- Anderson G (2010) Chronic Care: Making the Case for Ongoing Care. *Robert Wood Johnson Foundation* .
- Apple Inc (2022) Understanding Reference Frames and Device Attitude | Apple Developer Documentation. *Apple Developer* .
- Bardhan I, Chen H, Karahanna E (2017) The Role of Information Systems and Analytics in Chronic Disease Prevention and Management. *MIS Quarterly* .
- Bockting CL, Hollon SD, Jarrett RB, Kuyken W, Dobson K (2015) A lifetime approach to major depressive disorder: The contributions of psychological interventions in preventing relapse and recurrence. *Clinical Psychology Review* 41:16–26.
- Bot BM, Suver C, Neto EC, Kellen M, Klein A, Bare C, Doerr M, Pratap A, Wilbanks J, Dorsey ER, Friend SH, Trister AD (2016) The mPower study, Parkinson disease mobile data collected using ResearchKit. *Scientific Data* 3(1):1–9.
- Canzian L, Musolesi M (2015) Trajectories of depression: unobtrusive monitoring of depressive states by means of smartphone mobility traces analysis. *Proceedings of the 2015 ACM International Joint Conference on Pervasive and Ubiquitous Computing*.
- Caruana R, Lou Y, Gehrke J, Koch P, Sturm M, Elhadad N (2015) Intelligible Models for HealthCare: Predicting Pneumonia Risk and Hospital 30-day Readmission. *Proceedings of KDD* Place: New York, NY, USA Publisher: ACM.
- CDC (2012) Mental Health and Chronic Diseases CDC Fact Sheet. Technical report.
- CDC (2021) U.S. healthcare spending attributable to cigarette smoking in 2014. *CDC* 150.
- CDC (2022) Chronic Diseases in America. *CDC* .
- Chai S, Das S, Rao HR (2011) Factors Affecting Bloggers’ Knowledge Sharing: An Investigation Across Gender. *Journal of Management Information Systems* 28(3):309–342.
- Chen C, Li O, Tao C, Barnett AJ, Su J, Rudin C (2019) This Looks Like That: Deep Learning for Interpretable Image Recognition. *Proceedings of the 33rd International Conference on Neural Information Processing Systems*.
- Cheng HT, Koc L, Harmsen J, Shaked T, Chandra T, Aradhye H, Anderson G, Corrado G, Chai W, Ispir M, Anil R, Haque Z, Hong L, Jain V, Liu X, Shah H (2016) Wide & deep learning for recommender systems.

- Cho K, Van Merriënboer B, Bahdanau D, Bengio Y (2014) On the Properties of Neural Machine Translation: Encoder-Decoder Approaches.
- Coelln Rv, Dawe RJ, Leurgans SE, Curran TA, Truty T, Yu L, Barnes LL, Shulman JM, Shulman LM, Bennett DA, Hausdorff JM, Buchman AS (2019) Quantitative mobility metrics from a wearable sensor predict incident parkinsonism in older adults. *Parkinsonism & Related Disorders* 65:190–196.
- Czech MD, Patel S (2019) GaitPy: An Open-Source Python Package for Gait Analysis Using an Accelerometer on the Lower Back. *Journal of Open Source Software* 4(43):1778.
- Dadkhah M, Mehraeen M, Rahimnia F, Kimiafar K (2021) Use of internet of things for chronic disease management: An overview. *Journal of Medical Signals & Sensors* 11(2):138–138.
- Dattani S, Ritchie H, Roser M (2021) Mental Health. *Our World in Data* .
- Dias D, Cunha JPS (2018) Wearable Health Devices—Vital Sign Monitoring, Systems and Technologies. *Sensors* 18(8):2414–2414.
- Dixon-Woods M, Redwood S, Leslie M, Minion J, Martin GP, Coleman JJ (2013) Improving quality and safety of care using "technovigilance": an ethnographic case study of secondary use of data from an electronic prescribing and decision support system. *The Milbank Quarterly* 91(3):424–454.
- Farhan AA, Yue C, Morillo R, Ware S, Lu J, Bi J, Kamath J, Russell A, Bamis A, Wang B (2016) Behavior vs. introspection: refining prediction of clinical depression via smartphone sensing data. *2016 IEEE Wireless Health (WH)*.
- Goodfellow I, Bengio Y, Courville A (2016) *Deep Learning* (The MIT Press).
- Hase P, Chen C, Li O, Rudin C (2019) Interpretable Image Recognition with Hierarchical Prototypes. *Proceedings of the AAAI Conference on Human Computation and Crowdsourcing* 7:32–40.
- Heslin M, Jin H, Trevillion K, Ling X, Nath S, Barrett B, Demilew J, Ryan EG, O'Connor S, Sands P, Milgrom J, Bick D, Stanley N, Hunter MS, Howard LM, Byford S (2022) Cost-effectiveness of screening tools for identifying depression in early pregnancy: a decision tree model. *BMC Health Services Research* 22(1):774.
- Hubble RP, Naughton GA, Silburn PA, Cole MH (2015) Wearable Sensor Use for Assessing Standing Balance and Walking Stability in People with Parkinson's Disease: A Systematic Review. *PLOS ONE* 10(4):e0123705.
- Jacobson NC, Chung YJ (2020) Passive Sensing of Prediction of Moment-To-Moment Depressed Mood among Undergraduates with Clinical Levels of Depression Sample Using Smartphones. *Sensors* 20(12):3572.
- Karahanna E, Bardhan I, Chen H (2020) Connecting systems, data, and people: A multidisciplinary research roadmap for chronic disease management. *MIS Quarterly* 44(1):185–200.
- Katon WJ, Lin EH, Von Korff M, Ciechanowski P, Ludman EJ, Young B, Peterson D, Rutter CM, McGregor M, McCulloch D (2010) Collaborative Care for Patients with Depression and Chronic Illnesses. *New England Journal of Medicine* 363(27):2611–2620.

-
- Kingma DP, Ba J (2015) Adam: A method for stochastic optimization. *International Conference on Learning Representations*, URL <http://arxiv.org/abs/1412.6980>.
- Laplante PA, Laplante NL (2015) A Structured approach for describing healthcare applications for the Internet of Things. *IEEE World Forum on Internet of Things* 621–625.
- Lee J, Hong M, Ryu S (2015) Sleep Monitoring System Using Kinect Sensor:. *International Journal of Distributed Sensor Networks* 2015.
- Lemke MR, Wendorff T, Mieth B, Buhl K, Linnemann M (2000) Spatiotemporal gait patterns during over ground locomotion in major depression compared with healthy controls. *Journal of Psychiatric Research* 34(4-5):277–283.
- Lundberg SM, Lee SI (2017) A Unified Approach to Interpreting Model Predictions.
- Luo W, Li Y, Urtasun R, Zemel R (2016) Understanding the effective receptive field in deep convolutional neural networks. *Proceedings of the 30th International Conference on Neural Information Processing Systems* (Red Hook, NY, USA: Curran Associates Inc.), 4905–4913, NIPS’16, ISBN 978-1-5108-3881-9.
- Marsh L (2013) Depression and Parkinson’s Disease: Current Knowledge. *Current neurology and neuroscience reports* 13(12):409–409.
- Martin MS, Wells GA, Crocker AG, Potter BK, Colman I (2017) Decision curve analysis as a framework to estimate the potential value of screening or other decision-making aids. *International Journal of Methods in Psychiatric Research* 27(1):e1601.
- Mayo Clinic MC (2022) Depression (major depressive disorder) - Symptoms and causes.
- Michalak J, Troje NF, Fischer J, Vollmar P, Heidenreich T, Schulte D (2009) Embodiment of sadness and depression-gait patterns associated with dysphoric mood. *Psychosomatic Medicine* 71(5):580–587.
- Millor N, Lecumberri P, Gómez M, Martínez A, Martinikorena J, Rodríguez-Mañas L, García-García FJ, Izquierdo M (2017) Gait Velocity and Chair Sit-Stand-Sit Performance Improves Current Frailty-Status Identification. *IEEE Transactions on Neural Systems and Rehabilitation Engineering* 25(11):2018–2025.
- Ming Y, Xu P, Qu H, Ren L (2019) Interpretable and Steerable Sequence Learning via Prototypes. *Proceedings of the 25th ACM SIGKDD International Conference on Knowledge Discovery & Data Mining*.
- Moon S, Song HJ, Sharma VD, Lyons KE, Pahwa R, Akinwuntan AE, Devos H (2020) Classification of Parkinson’s disease and essential tremor based on balance and gait characteristics from wearable motion sensors via machine learning techniques: a data-driven approach. *Journal of NeuroEngineering and Rehabilitation* 17(1):125.
- Moss L, Corsar D, Shaw M, Piper I, Hawthorne C (2022) Demystifying the Black Box: The Importance of Interpretability of Predictive Models in Neurocritical Care. *Neurocritical Care* 37(2):185–191.
- Mozaffari N, Rezazadeh J, Farahbakhsh R, Yazdani S, Sandrasegaran K (2019) Practical fall detection based on IoT technologies: A survey. *Internet of Things* 8:100124–100124.

- Murphy KP (2022) *Probabilistic Machine Learning: An Introduction* (The MIT Press).
- Nauta M, Bree Rv, Seifert C (2021a) Neural Prototype Trees for Interpretable Fine-Grained Image Recognition. *IEEE Conference on Computer Vision and Pattern Recognition*.
- Nauta M, Jutte A, Provoost J, Seifert C (2021b) This Looks Like That, Because ... Explaining Prototypes for Interpretable Image Recognition. *Machine Learning and Principles and Practice of Knowledge Discovery in Databases*.
- Nemati E, Rahman MJ, Blackstock E, Nathan V, Rahman MM, Vatanparvar K, Kuang J (2020) Estimation of the Lung Function Using Acoustic Features of the Voluntary Cough. *2020 42nd Annual International Conference of the IEEE Engineering in Medicine & Biology Society (EMBC)*.
- NHS (2022) Symptoms - Clinical depression. *National Health Service* .
- NIH (2022) Chronic Illness and Mental Health: Recognizing and Treating Depression. *National Institute of Mental Health* .
- Oung Q, Hariharan M, Lee H, Basah S, Sarillee M, Lee C (2015) Wearable multimodal sensors for evaluation of patients with Parkinson disease. *2015 IEEE International Conference on Control System, Computing and Engineering (ICCSCE)*.
- Padmanabhan B, Fang X, Sahoo N, Burton-Jones A (2022) Machine Learning in Information Systems Research. *MIS Quarterly* 46(1):iii–xix.
- Patient (2022) PHQ-9 Depression Test Questionnaire. *patient.info* .
- Piau A, Mattek N, Crissey R, Beattie Z, Dodge H, Kaye J (2020) When Will My Patient Fall? Sensor-Based In-Home Walking Speed Identifies Future Falls in Older Adults. *The Journals of Gerontology: Series A* 75(5):968–973.
- Polat K (2019) A Hybrid Approach to Parkinson Disease Classification Using Speech Signal: The Combination of SMOTE and Random Forests. *2019 Scientific Meeting on Electrical-Electronics & Biomedical Engineering and Computer Science (EBBT)*.
- Rai A (2017) Editor’s comments: diversity of Design Science Research. *MIS Quarterly* 41(1):iii–xviii.
- Rampell C (2013) The Half-Trillion-Dollar Depression. *The New York Times* .
- Rastegari E, Azizian S, Ali H (2019) Machine Learning and Similarity Network Approaches to Support Automatic Classification of Parkinson’s Diseases Using Accelerometer-based Gait Analysis. *Hawaii International Conference on System Sciences 2019 (HICSS-52)* .
- Reijnders JS, Ehrt U, Weber WE, Aarsland D, Leentjens AF (2008) A systematic review of prevalence studies of depression in Parkinson’s disease. *Movement Disorders* 23(2):183–189.
- Rymarczyk D, Struski L, Tabor J, Zieliński B (2021) ProtoPShare: Prototypical Parts Sharing for Similarity Discovery in Interpretable Image Classification.

-
- Shitole V, Li F, Kahng M, Tadepalli P, Fern A (2021) One Explanation is Not Enough: Structured Attention Graphs for Image Classification. *Advances in Neural Information Processing Systems*.
- Sigcha L, Costa N, Pavón I, Costa S, Arezes P, López JM, De Arcas G (2020) Deep Learning Approaches for Detecting Freezing of Gait in Parkinson’s Disease Patients through On-Body Acceleration Sensors. *Sensors 2020, Vol. 20, Page 1895* 20(7):1895–1895.
- Simchi-Levi D (2020) From the editor. *Management Science* 66(1):1–4.
- Singh G, Yow KC (2021) These do not Look like Those: An Interpretable Deep Learning Model for Image Recognition. *IEEE Access* 9:41482–41493.
- Sloman L, Berridge M, Homatidis S, Hunter D, Duck T (1982) Gait patterns of depressed patients and normal subjects. *American Journal of Psychiatry* 139(1):94–97.
- Statista (2022) Topic: US smartphone market.
- Um TT, Pfister FMJ, Pichler D, Endo S, Lang M, Hirche S, Fietzek U, Kulić D (2017) Data augmentation of wearable sensor data for parkinson’s disease monitoring using convolutional neural networks. *Proceedings of the 19th ACM International Conference on Multimodal Interaction*.
- Vancampfort D, Basangwa D, Kimbowa S, Firth J, Schuch F, Van Damme T, Mugisha J (2020) Test–retest reliability, validity, and correlates of the 2-min walk test in outpatients with depression. *Physiotherapy Research International* 25(2):e1821–e1821.
- Wang B, Di Buccio E, Melucci M (2021a) Word2Fun: Modelling Words as Functions for Diachronic Word Representation. *Advances in Neural Information Processing Systems*.
- Wang J, Liu H, Wang X, Jing L (2021b) Interpretable Image Recognition by Constructing Transparent Embedding Space.
- Watanabe A, Noguchi H, Oe M, Sanada H, Mori T (2017) Development of a Plantar Load Estimation Algorithm for Evaluation of Forefoot Load of Diabetic Patients during Daily Walks Using a Foot Motion Sensor. *Journal of Diabetes Research* 2017:e5350616.
- Xie J, Liu X (2020) Unbox the Blackbox: Predict and Interpret YouTube Viewership Using Deep Learning. *arXiv* .
- Xie J, Liu X, Zeng D, Fang X (2022) Understanding Medication Nonadherence from Social Media: A Sentiment-Enriched Deep Learning Approach. *MIS Quarterly* 46(1):341–372.
- Xu D, Ruan C, Körpeoglu E, Kumar S, Achan K (2020a) Inductive representation learning on temporal graphs. *8th International Conference on Learning Representations, ICLR 2020*.
- Xu W, Xian Y, Wang J, Schiele B, Akata Z (2020b) Attribute Prototype Network for Zero-Shot Learning. *Advances in Neural Information Processing Systems*.
- Yu S, Chai Y, Chen H, Sherman SJ, Brown RA (2022) Wearable Sensor-based Chronic Condition Severity Assessment: An Adversarial Attention-based Deep Multisource Multitask Learning Approach. *MIS Quarterly* Forthcoming.

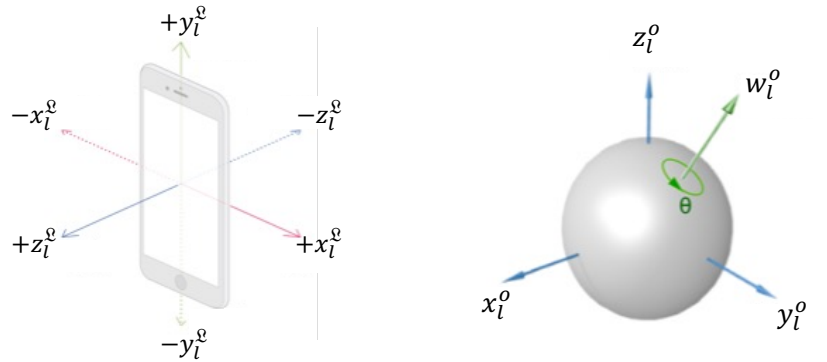
Zhang H, Deng K, Li H, Albin RL, Guan Y (2020) Deep Learning Identifies Digital Biomarkers for Self-Reported Parkinson's Disease. *Patterns* 1(3):100042.

Zhu H, Samtani S, Brown RA, Chen H (2021) A deep learning approach for recognizing activity of daily living (adl) for senior care: Exploiting interaction dependency and temporal patterns. *MIS Quarterly* 45(2):859–896.

Supplementary Materials

A. The Definition of Sensor Features

We explain the content of a sensor feature as mentioned in Section 3. At each timepoint l , the mobile sensor collects accelerometer readings $[x_l^{\mathfrak{L}}, y_l^{\mathfrak{L}}, z_l^{\mathfrak{L}}]$ and orientation readings $[x_l^{\mathfrak{O}}, y_l^{\mathfrak{O}}, z_l^{\mathfrak{O}}, w_l^{\mathfrak{O}}]$. A graphic illustration of these sensor readings is shown in Figure A.1.



Left: $[x_l^{\mathfrak{L}}, y_l^{\mathfrak{L}}, z_l^{\mathfrak{L}}]$ measures the acceleration readings along the x, y, z axes in the local reference frame.

Right: $[x_l^{\mathfrak{O}}, y_l^{\mathfrak{O}}, z_l^{\mathfrak{O}}, w_l^{\mathfrak{O}}]$ measures the movement and rotation of the local reference frame relative to the global reference frame. The local reference frame is fixed to the mobile device, and moves and rotates along with the device.

The local reference frame is the coordinate system of the mobile device. The axis of local reference frame changes relative to the earth when the device's orientation changes. The global reference frame is the coordinate system when the device is placed horizontally and the device's x axis points to magnetic north. Therefore, the global reference frame is fixed to the earth regardless the device moves or not.

Figure A.1 Sensor Readings (Apple Inc 2022)

The accelerometer readings are in the local reference frame, which most existing studies rely on (Piau et al. 2020, Yu et al. 2022, Zhu et al. 2021). However, these local reference readings do not reflect the precise walking pattern in the geographic coordinate system, because it moves and rotates along with the mobile device. To address this issue and make the interpretation more meaningful in the geographic sense, we decide to work with the readings in the global reference frame. We transform the local reference frame accelerometer vector $v_l^{\mathfrak{L}} = [x_l^{\mathfrak{L}}, y_l^{\mathfrak{L}}, z_l^{\mathfrak{L}}]^T$ to the global reference frame as $v_l^{\mathfrak{G}} = [x_l^{\mathfrak{G}}, y_l^{\mathfrak{G}}, z_l^{\mathfrak{G}}]^T$ via the quaternion rotation

$$v_l^{\mathfrak{G}} = \mathcal{R}_l v_l^{\mathfrak{L}}$$

where \mathcal{R}_l is the rotation matrix derived from quaternion $[x_l^o, y_l^o, z_l^o, w_l^o]$ as follows. In general, given a quaternion $[x, y, z, w]$, the corresponding rotation matrix \mathcal{R} is defined as⁹

$$\mathcal{R} = \begin{bmatrix} w^2 + x^2 - y^2 - z^2 & 2xy - 2wz & 2xz + 2wy \\ 2xy + 2wz & w^2 - x^2 + y^2 - z^2 & 2yz - 2wx \\ 2xz - 2wy & 2yz + 2wx & w^2 - x^2 - y^2 + z^2 \end{bmatrix}. \quad (\text{EC.1})$$

Then, we define the sensor feature a_l as

$$a_l = [x_l^{\mathfrak{G}}, y_l^{\mathfrak{G}}, z_l^{\mathfrak{G}}]^T. \quad (\text{EC.2})$$

Following the best practice of data augmentation for mobile sensor data (Um et al. 2017, Zhang et al. 2020), during the training stage, we further transform the input sensor features with random rotations to improve the generalization ability of our model. To do this, we first sample a quaternion using Algorithm 2 where $\text{Uniform}(b_1, b_2)$ means the uniform distribution on the interval $[b_1, b_2]$, and then plug the obtained quaternion into Equation EC.1 to construct a random rotation matrix. Within each training epoch and for each walking test, we construct a random rotation matrix $\tilde{\mathcal{R}}$ as described, and then use it to transform all sensor features of the walking test as $\langle \tilde{\mathcal{R}}a_1, \tilde{\mathcal{R}}a_2, \dots, \tilde{\mathcal{R}}a_L \rangle$. Once the training stage is finished, we use the original sensor features $\langle a_1, a_2, \dots, a_L \rangle$ to do inference.

Algorithm 2 Sample a Quaternion

- 1: Draw $x \sim \text{Uniform}(0, 1)$, $y \sim \text{Uniform}(0, 1)$, $z \sim \text{Uniform}(0, 1)$.
 - 2: Let $\text{norm} = \sqrt{x^2 + y^2 + z^2}$, and set $x = x/\text{norm}$, $y = y/\text{norm}$, $z = z/\text{norm}$.
 - 3: Draw $\theta \sim \text{Uniform}(0, 2\pi)$.
 - 4: Set $w = \cos(\theta/2)$, $x = x \sin(\theta/2)$, $y = y \sin(\theta/2)$, $z = z \sin(\theta/2)$
 - 5: Return $[x, y, z, w]$
-

⁹https://en.wikipedia.org/wiki/Quaternions_and_spatial_rotation

B. The Specification of the Feature Extraction Layer

Recall that X_i denotes the sequence of sensor features of the i th walking test performed by a focal patient. In this section, we focus on extracting the feature matrix H_i^S from a single waling test, and therefore drop the subscript i to simplify the notation. We partition X into three segments according to in which task the sensor signals are recorded. Namely, $X = [X_1, X_2, X_3]$, which respectively denote the segment for the outbound, return, and rest (standing still) tasks. According to the definition of sensor features given in Appendix A, each segment X_j is in fact a matrix of size $3 \times L_j$ for $j = 1, 2, 3$, where L_j is the length of segment j . In general, different segments have different lengths in different walking tests. In what follows, we assume that X has been downsampled with the frequency of 10 Hz, while the treatment of other sampling frequencies should be adjusted proportionally.

Under the sampling frequency of 10 Hz, we observe that the rest segment on average has the longest sequence, with $L_3 = 296$ by averaging over all walking tests. To facilitate batch training, we reshape each segment into a matrix of size 3×300 , by either padding it with zero columns if its length is smaller than 300, or discarding the extra columns if its length is larger than 300. After the reshaping step, we treat each segment X_j as an input of 3 channels and length 300, and then use the same CNN layer to extract a feature matrix of size 128×5 from X_j . The CNN layer is composed by a sequence of one-dimensional convolution (Conv1d) layers, each followed in order by a one-dimensional batch normalization layer (BatchNorm1d), a max pooling layer (MaxPool1d), and lastly a leaky ReLU layer (LeakyReLU) with slope 0.01 for non-linear activation (Goodfellow et al. 2016). Following the style of Zhu et al. (2021), we report the detailed architecture of the CNN layer in Table A.1. Since the BatchNorm1d layer and the LeakyReLU layer do not change the input shape, we do not list them in Table A.1. After the last Conv1d layer in Table A.1, we do not add the MaxPool1d layer nor the LeakyReLU layer.

Table A.1 The Specification of the CNN Layer

	Kernel Size	Stride	Output Channel	Output Shape
Conv1d	8	1	256	(256, 293)
MaxPool1d	2	2		(256, 146)
Conv1d	8	1	512	(512, 139)
MaxPool1d	2	2		(512, 69)
Conv1d	8	1	256	(256, 62)
MaxPool1d	2	2		(256, 31)
Conv1d	8	1	128	(128, 24)
MaxPool1d	2	2		(128, 12)
Conv1d	8	1	128	(128, 5)

Given the input $X = [X_1, X_2, X_3]$, we feed each segment X_j into the same CNN layer specified above, and obtain a feature matrix $H_j^{\mathbb{S}}$ of size 128×5 for $j = 1, 2, 3$. We then horizontally concatenate these feature matrices to obtain the final feature matrix as $H^{\mathbb{S}} = [H_1^{\mathbb{S}}, H_2^{\mathbb{S}}, H_3^{\mathbb{S}}]$ of size $n_e \times n_o$, where $n_e = 128$ and $n_o = 15$.

C. The Density Function of the Logistic-Normal Distribution

We employ the change of variables formula (Murphy 2022) to derive Equation 8, which in general states that if a random vector $x \in R^M$ is mapped to another random vector $z \in R^M$ by an invertible function f , i.e., $z = f(x)$, then the density function of z , denoted by $p_z(z)$, is related to the density function of x , denoted by $p_x(x)$, by the following relationship:

$$p_z(z) = p_x(g(z)) |\det[J_g(z)]| \quad (\text{EC.3})$$

where g is the inverse function of f , $J_g(z) \in R^{M \times M}$ is the Jacobian matrix of g evaluated at z , $\det[\cdot]$ is the matrix determinant operator, and $|\cdot|$ is the absolute value operator.

In our case, $z = \sigma(x)$, which means that $f = \sigma$ and $g = \sigma^{-1}$. Using the fact that $\partial x_m / \partial z_m = 1 / (z_m(1 - z_m))$, the corresponding Jacobian matrix can be computed as

$$J_g(z) = \begin{pmatrix} \frac{1}{z_1(1-z_1)} & 0 & \cdots & 0 \\ 0 & \frac{1}{z_2(1-z_2)} & \cdots & 0 \\ \vdots & \vdots & \ddots & \vdots \\ 0 & 0 & \cdots & \frac{1}{z_M(1-z_M)} \end{pmatrix}, \quad (\text{EC.4})$$

which is a diagonal matrix because σ^{-1} has been element-wisely applied on z . Given that $0 < z_m < 1$ for $m = 1, 2, \dots, M$, all the diagonal elements are positive, and thus we have

$$|\det[J_g(z)]| = \frac{1}{\prod_{m=1}^M z_m(1 - z_m)}. \quad (\text{EC.5})$$

Recall that $x \sim \mathcal{N}(\mu, \Sigma)$, then the corresponding density function is given by

$$p_x(x) = \frac{\exp\left(-\frac{1}{2}(x - \mu)^T \Sigma^{-1}(x - \mu)\right)}{\sqrt{(2\pi)^M \det[\Sigma]}}. \quad (\text{EC.6})$$

Plugging Equation EC.5 and EC.6 into Equation EC.3, and setting $x = \sigma^{-1}(z)$, we obtain Equation 8.

D. Manually Crafted Features for Benchmarks

Recall that given a walking test, we observe a sequence of sensor signals $\langle v_1^{\mathfrak{L}}, v_2^{\mathfrak{L}}, \dots, v_L^{\mathfrak{L}} \rangle$, where $v_l^{\mathfrak{L}}$ is the accelerometer readings recorded in the local reference frame at timepoint l , as explained in Appendix A. To simplify notation, we drop the superscript \mathfrak{L} , and write $v_l = [v_{x,l}, v_{y,l}, v_{z,l}]^T$. Following Yu et al. (2022), we define the following features for each given walking test.

Table A.2 Features for Conventional Machine Learning Models

Feature Name	Formula
Mean x-axis values	$u_x = \frac{1}{L} \sum_{l=1}^L v_{x,l}$
Mean y-axis values	$u_y = \frac{1}{L} \sum_{l=1}^L v_{y,l}$
Mean z-axis values	$u_z = \frac{1}{L} \sum_{l=1}^L v_{z,l}$
St. D. of x-axis values	$\sigma_x = \sqrt{\frac{1}{L-1} \sum_{l=1}^L (v_{x,l} - u_x)^2}$
St. D. of y-axis values	$\sigma_y = \sqrt{\frac{1}{L-1} \sum_{l=1}^L (v_{y,l} - u_y)^2}$
St. D. of z-axis values	$\sigma_z = \sqrt{\frac{1}{L-1} \sum_{l=1}^L (v_{z,l} - u_z)^2}$
Mean magnitude	$u_v = \frac{1}{L} \sum_{l=1}^L \ v_l\ , \ v_l\ = \sqrt{v_{x,l}^2 + v_{y,l}^2 + v_{z,l}^2}$
St. D. of magnitude	$\sigma_v = \sqrt{\frac{1}{L-1} \sum_{l=1}^L (\ v_l\ - u_v)^2}$
Mean x-axis jerk	$\alpha_x = \frac{1}{L-1} \sum_{l=1}^{L-1} d_{x,l}$, where $d_{x,l} = v_{x,l+1} - v_{x,l}$
Mean y-axis jerk	$\alpha_y = \frac{1}{L-1} \sum_{l=1}^{L-1} d_{y,l}$, where $d_{y,l} = v_{y,l+1} - v_{y,l}$
Mean z-axis jerk	$\alpha_z = \frac{1}{L-1} \sum_{l=1}^{L-1} d_{z,l}$, where $d_{z,l} = v_{z,l+1} - v_{z,l}$
St. D. of x-axis jerk	$\beta_x = \sqrt{\frac{1}{L-2} \sum_{l=1}^{L-1} (d_{x,l} - \alpha_x)^2}$
St. D. of y-axis jerk	$\beta_y = \sqrt{\frac{1}{L-2} \sum_{l=1}^{L-1} (d_{y,l} - \alpha_y)^2}$
St. D. of z-axis jerk	$\beta_z = \sqrt{\frac{1}{L-2} \sum_{l=1}^{L-1} (d_{z,l} - \alpha_z)^2}$
Mean jerk magnitude	$\alpha_d = \frac{1}{L-1} \sum_{l=1}^{L-1} \ d_l\ $, where $\ d_l\ = \sqrt{d_{x,l}^2 + d_{y,l}^2 + d_{z,l}^2}$
St. D. of jerk magnitude	$\beta_d = \sqrt{\frac{1}{L-2} \sum_{l=1}^{L-1} (\ d_l\ - \alpha_d)^2}$
Stride time variability on x-axis	(1) Identify signal peaks in x-axis, $[t_1, t_2, \dots, t_Q]$; (2) Identify stride times $[dt_1, dt_2, \dots, dt_{Q-1}]$, where $dt_i = t_{i+1} - t_i$; (3) Compute stride time variability $V_x = \sqrt{\frac{1}{Q-2} \sum_{i=1}^{Q-1} (dt_i - \overline{dt})^2}$
Stride time variability on y-axis	(1) Identify signal peaks in y-axis, $[t_1, t_2, \dots, t_Q]$; (2) Identify stride times $[dt_1, dt_2, \dots, dt_{Q-1}]$, where $dt_i = t_{i+1} - t_i$; (3) Compute stride time variability $V_y = \sqrt{\frac{1}{Q-2} \sum_{i=1}^{Q-1} (dt_i - \overline{dt})^2}$
Stride time variability on z-axis	(1) Identify signal peaks in z-axis, $[t_1, t_2, \dots, t_Q]$; (2) Identify stride times $[dt_1, dt_2, \dots, dt_{Q-1}]$, where $dt_i = t_{i+1} - t_i$; (3) Compute stride time variability $V_z = \sqrt{\frac{1}{Q-2} \sum_{i=1}^{Q-1} (dt_i - \overline{dt})^2}$
Stride time vairability on magnitude	(1) Identify signal peaks in magnitude, $[t_1, t_2, \dots, t_Q]$; (2) Identify stride times $[dt_1, dt_2, \dots, dt_{Q-1}]$, where $dt_i = t_{i+1} - t_i$; (3) Compute stride time variability $V_v = \sqrt{\frac{1}{Q-2} \sum_{i=1}^{Q-1} (dt_i - \overline{dt})^2}$

E. Factor Loadings of the Trust Scale

Table A.3 Factor Loadings of the Trust Scale

Factor	Loading
Trust 1	0.533
Trust 2	0.993
Trust 3	0.759
Trust 4	0.620
Trust 5	0.805
Trust 6	0.798
Trust 7	0.946
Trust 8	0.933
Trust 9	0.932

References

- Goodfellow I, Bengio Y, Courville A (2016) *Deep Learning* (The MIT Press).
- Murphy KP (2022) *Probabilistic Machine Learning: An Introduction* (The MIT Press).
- Piau A, Mattek N, Crissey R, Beattie Z, Dodge H, Kaye J (2020) When Will My Patient Fall? Sensor-Based In-Home Walking Speed Identifies Future Falls in Older Adults. *The Journals of Gerontology: Series A* 75(5):968–973.
- Um TT, Pfister FMJ, Pichler D, Endo S, Lang M, Hirche S, Fietzek U, Kulić D (2017) Data augmentation of wearable sensor data for parkinson’s disease monitoring using convolutional neural networks. *Proceedings of the 19th ACM International Conference on Multimodal Interaction*.
- Yu S, Chai Y, Chen H, Sherman SJ, Brown RA (2022) Wearable Sensor-based Chronic Condition Severity Assessment: An Adversarial Attention-based Deep Multisource Multitask Learning Approach. *MIS Quarterly* Forthcoming.
- Zhang H, Deng K, Li H, Albin RL, Guan Y (2020) Deep Learning Identifies Digital Biomarkers for Self-Reported Parkinson’s Disease. *Patterns* 1(3):100042.
- Zhu H, Samtani S, Brown RA, Chen H (2021) A deep learning approach for recognizing activity of daily living (adl) for senior care: Exploiting interaction dependency and temporal patterns. *MIS Quarterly* 45(2):859–896.